

Chapter 2

The Synthesis and Reactivity of Group 7 Carbonyl Derivatives Relevant to Synthesis Gas Conversion

Abstract

Various Group 7 carbonyl complexes have been synthesized. Reduction of these complexes with hydride sources, such as LiHBEt_3 , led to the formation of formyl species. A more electrophilic carbonyl precursor, $[\text{Mn}(\text{PPh}_3)(\text{CO})_5][\text{BF}_4]$, reacted with transition metal hydrides to form a highly reactive formyl product. Moreover, a diformyl species was obtained when $[\text{Re}(\text{CO})_4(\text{P}(\text{C}_6\text{H}_4(p\text{-CF}_3))_3)_2][\text{BF}_4]$ was treated with excess LiHBEt_3 . The synthesis and reactivity of novel borane-stabilized Group 7 formyl complexes is also presented. The new carbene-like species display remarkable stability compared to the corresponding “naked” formyl complexes. Reactivity differs significantly whether BF_3 or $\text{B}(\text{C}_6\text{F}_5)_3$ binds the formyl oxygen. Unlike other analogs, $\text{Mn}(\text{CO})_3(\text{PPh}_3)_2(\text{CHOB}(\text{C}_6\text{F}_5)_3)$ is not stable over time and undergoes decomposition to a manganese carbonyl borohydride complex. Cationic Fischer carbenes were prepared by the reaction of the corresponding formyl species with electrophiles trimethylsilyl triflate and methyl triflate. While the siloxycarbene product is highly unstable at room temperature, the methoxycarbene is stable both in solution and in the solid state. Treating the methoxycarbene complexes with a hydride led to the formation of methoxymethyl species. Manganese methoxymethyl complexes are susceptible to $\text{S}_{\text{N}}2$ -type attack by a hydride to release dimethyl ether and a manganese anion, which presumably proceeds with further reaction with reactive impurities or borane present. Furthermore, subjecting manganese methoxymethyl complexes to an atmosphere of CO led to the formation of acyl products *via* migratory insertion. Mechanistic insight was obtained, which indicated that a manganese *bis*(phosphine) methoxymethyl requires initial loss of a phosphine by ligand

substitution before reaction is allowed to proceed. A dynamic exchange involving carbonylation/decarbonylation and isomerization processes is operational, leading to the presence of three products in equilibrium.

Introduction

Catalytic hydrogenation of carbon monoxide to hydrocarbons and oxygenates attracted much attention three decades ago due to the need to develop alternatives to petroleum feedstocks, although the origin of this interest can be traced back to well before World War II.¹ After the oil crisis of the seventies had receded and oil prices decreased significantly, active research in coal-related chemistry slowed down throughout the eighties and nineties. However, with proven petroleum supplies declining and oil prices constantly on the rise recently, renewed interest in the chemistry of carbon monoxide has emerged. Much like after the oil crisis, it is once again increasingly imperative to discover new methods for transforming alternate carbon feedstocks into hydrocarbons suitable for transportation fuel and other valuable chemicals. As such, coal and natural gas are becoming ever more attractive as sources of fuel (Figure 1). Moreover, current reserves of oil shale and tar sands are considerable in addition to resources obtained from biomass. Research pertaining to the transformation of coal and natural gas to energy is remarkably vast and spans over more than a century.² Synthesis gas, a mixture of carbon monoxide and hydrogen gas, is the principal intermediate involved during these transformations. It can be obtained commercially by several methods, mainly through coal gasification or steam methane reforming (Eqs. 1-4).



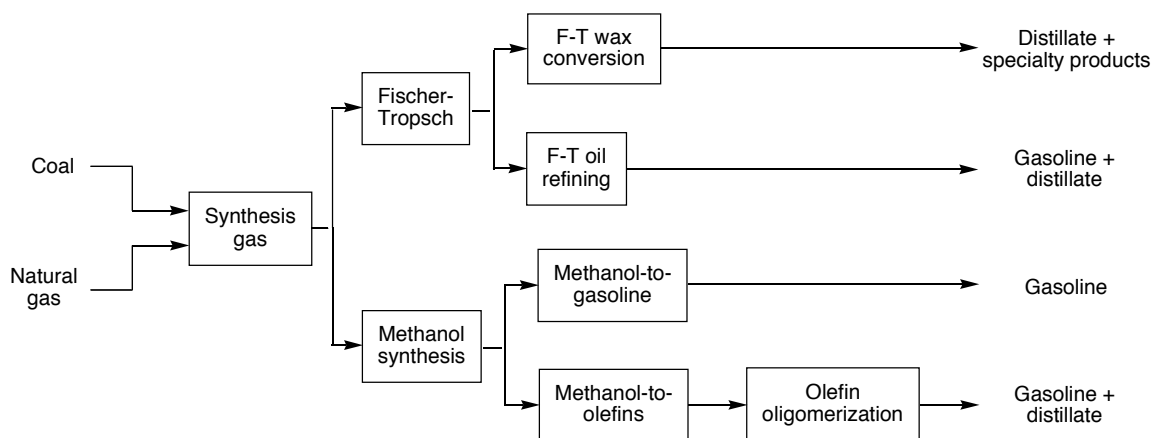
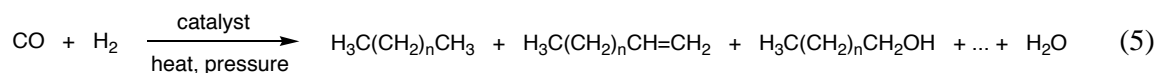


Figure 1. Routes to liquid fuels from coal and natural gas *via* synthesis gas (from ref. 2).

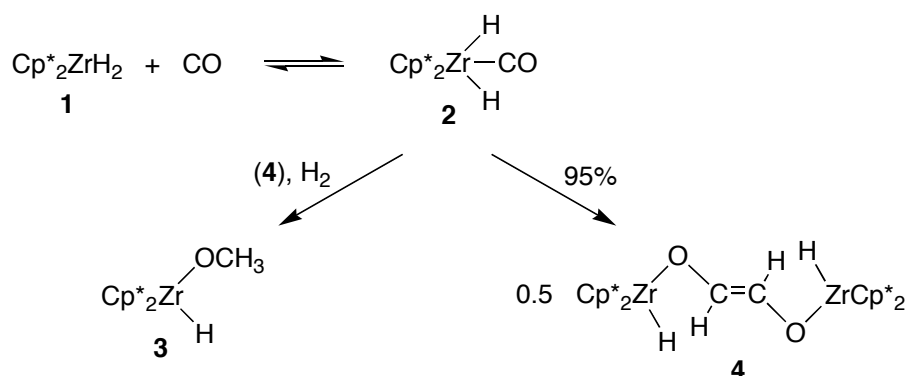
Extensive work has been accomplished in this field already using heterogeneous as well as homogeneous catalysts. With regards to heterogeneous catalysis, perhaps the most recognized process involving synthesis gas conversion to synthetic fuel and other chemicals is arguably the Fischer-Tropsch reaction. The Fischer-Tropsch reaction is an oligomerization reaction that converts synthesis gas into a complex mixture of hydrocarbons, olefins and various oxygenates (Eq. 5).³⁻⁶ Catalysts include iron and cobalt, both of which require alkali promoters, ruthenium for high molecular weight polymers and rhodium for low molecular weight oxygenated species. The Fischer-Tropsch process has been widely applied in South Africa since the 1950's using highly abundant coal as the raw material and more recently in Malaysia by Shell Oil using natural gas.



The industrial production of methanol from CO and H₂ also utilizes heterogeneous catalysts of various natures.⁷ A catalyst based on ZnO/Cr₂O₃ was widely used up to the late fifties, however the emergence of the highly active catalyst, CuO/ZnO, allowed the reaction to be carried out at much lower pressures and temperatures.¹ The most significant development in synthetic fuel technology since the discovery of the Fischer-Tropsch process is the Mobil methanol-to-gasoline (MTG) process. Methanol is efficiently converted to C₂-C₁₀ hydrocarbons in a reaction catalyzed by the synthetic zeolite ZSM-5.⁸

On the other hand, some of the best-studied systems have been homogeneous in nature. Solutions of HCo(CO)₄,⁹ and Ru(CO)₅,^{10,11} have been shown to catalyze the hydrogenation of CO to alcohols and formates. The same has been observed with mixtures of Cp₂ZrCl₂ and aluminum hydrides.¹² Of course, when discussing homogeneous reactions, one cannot omit the hydroformylation reaction, which converts olefins to aldehydes upon reaction with CO and H₂. This process is the oldest still in use today and responsible for producing the largest amount of material resulting from a homogeneous transition metal-catalyzed reaction.¹³ Homogeneous catalysis also allows selectivity to be achieved, as is the case in the synthesis of ethylene glycol from CO and H₂ using rhodium carbonyl clusters.¹⁴ Reactivity of zirconocene complexes has been promising in the preparation of ethylene glycol derivatives and other CO reduction products.¹⁵ The first report of such complexes involved in CO reduction was that of the hydrogenation of Cp*₂Zr(CO)₂ at 110 °C to give Cp*₂Zr(OCH₃)(H) (**3**).¹⁶ Additionally, reaction of Cp*₂ZrH₂ (**1**) with CO at -80 °C leads to the reversible formation of complex **2**, which upon warming to -50 °C generates dimeric complex **4** featuring a new C-C bond

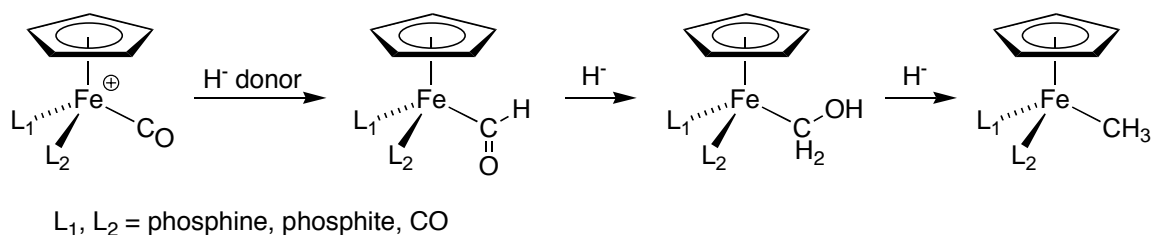
formed as the major product (Scheme 1).¹⁷ Interestingly, **4** could also be obtained by the reduction of the carbonyls from Cp*₂Zr(CO)₂ using **1** under H₂ at room temperature, demonstrating the potential of zirconium hydrides to act as hydride transfer agents.^{15,17} It was also shown that **1** could reduce other metal carbonyls, such as Group 5, 6 and 8 carbonyl complexes.^{18,19} Despite the remarkable reactivity of the zirconocene complexes, the high oxophilicity of zirconium precluded the development of a catalytic system based on these species, as the organic fragment could not easily be removed from the metal center.



Scheme 1. C-C bond formation using zirconocene derivatives.

Several other systems have enjoyed success in demonstrating reaction steps and potential intermediates believed to be relevant in key industrial processes. Among these, iron, rhenium and manganese systems have played an important role. Many iron complexes have been shown to participate in CO reduction chemistry and in particular, complexes of the type CpFeL₁L₂(CO)⁺ (L₁ and L₂ = phosphine, phosphite, or CO) were shown to generate formyl, hydroxymethyl and methyl species upon reduction (Scheme

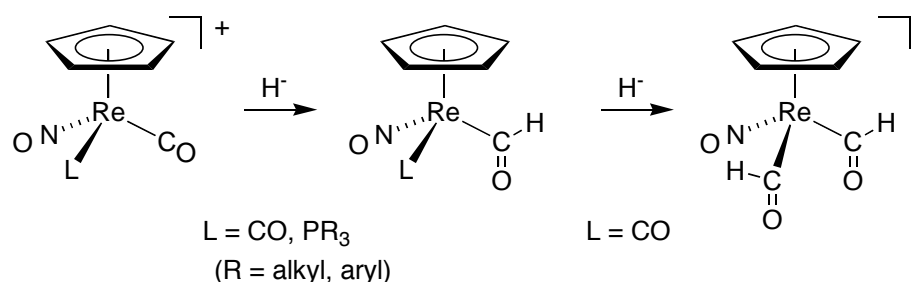
2).^{1,20-24} Additionally, the first reported formyl complex, $[(\text{Ph}_3\text{P})_2\text{N}][(\text{CO})_4\text{Fe}(\text{CHO})]$, was described by Collman and Winter in 1973.²⁵



Scheme 2. CO reduction chemistry using iron complexes.

Group 7 complexes have also been used to demonstrate similar steps. A system extensively studied by various research groups is based on an electrophilic rhenium carbonyl center supported by cyclopentadienyl-type ligands, a nitrosyl group and in some cases phosphines.²⁶⁻³⁰ As was mentioned earlier, formyl complexes are often suggested as the first important intermediate involved during catalytic CO reduction processes. Two formation pathways are possible. The first involves migratory insertion from a metal carbonyl hydride species. While such reaction is highly preceded with metal carbonyl alkyls to metal acyls, the carbonylation of metal hydrides to formyls is highly unfavorable. Nevertheless, it is worth noting the contribution from Wayland and coworkers, who demonstrated the reversible carbonylation of $\text{Rh}(\text{OEP})(\text{H})$ (OEP = octaethylporphyrin) to an isolable neutral formyl $\text{Rh}(\text{OEP})(\text{CHO})$.³¹ Marks and coworkers also reported on the migratory CO insertion into metal-hydrogen bonds to produce mononuclear formyls using organoactinide species.³² The second and most common pathway to formyls, as was shown in examples above, involves hydride attack upon a coordinated CO ligand. This process is facilitated by increasing the

electrophilicity of the carbonyl ligand. The rhenium carbonyl systems studied by Casey, Gladysz and others exhibit high electrophilicity, which can even allow a second reduction to form an isolable diformyl species from $[\text{CpRe}(\text{NO})(\text{CO})_2][\text{X}]$ ($\text{X} = \text{BF}_4, \text{PF}_6$) (IR: $\nu_{\text{CO}} = 2115, 2060 \text{ cm}^{-1}$) (Scheme 3).^{26,33,34} A convenient but empirical method of evaluating the electrophilicity of a metal carbonyl complex is to measure the CO stretching frequency of the terminal CO ligands. A more electron-deficient metal center will generate less backbonding into the CO π^* orbital, shortening the C-O bond distance and causing high stretching frequencies in the IR spectrum. The polarization of the C-O bond induced renders the carbonyl carbon more susceptible to hydride (and other nucleophilic) attack.



Scheme 3. Synthesis of a rhenium diformyl species.

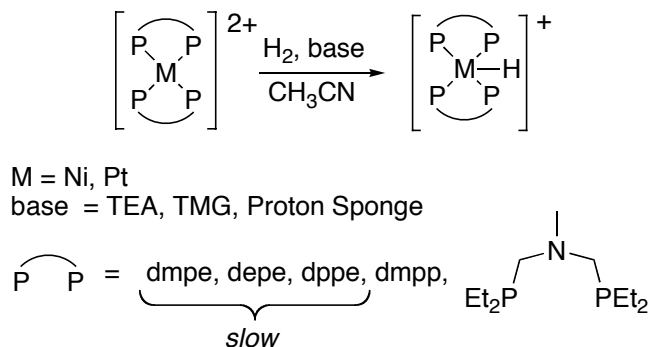
Other Group 7 systems have proved quite promising, such as complexes of the type $[\text{M}(\text{L})(\text{PPh}_3)(\text{CO})_4][\text{BF}_4]$ ($\text{M} = \text{Mn, Re}$; $\text{L} = \text{CO}, \text{PPh}_3$) studied by Gibson and coworkers.³⁵⁻³⁸ These complexes react in a similar fashion as discussed above to give formyl, Fischer carbene and alkoxymethyl species. It is worth noting however that because these carbonyl precursors are not as electron-deficient as the cyclopentadienyl rhenium carbonyl complexes discussed earlier ($\nu_{\text{CO}} = 2001$ and 2000 cm^{-1} for

[Mn(PPh₃)₂(CO)₄][BF₄] and [Re(PPh₃)₂(CO)₄][BF₄], respectively), they have only been shown to be reduced by main group hydrides, and not by transition metal hydrides (discussed in the next paragraph). Nevertheless, this ligand framework is very convenient because it allows for high tunability, simply by changing the steric and electronic character as well as the number of phosphine ligands coordinated to the metal center.

While most of the discussion so far has focused on the carbonyl reduction side of the problem, an equally important aspect regards the ability to use H₂ as the hydride and proton source for carbon monoxide reduction. Tremendous work has been achieved already, as was described above, in demonstrating key steps relevant to the conversion of carbon monoxide to chemicals, however most of these steps were carried out using stoichiometric reagents. Recently, DuBois and coworkers developed late transition metal hydrides capable of acting as hydride transfer agents (Eq. 6).²⁹ When certain requirements are met, such metal hydrides can also be generated from the heterolytic cleavage of H₂, typically with the help of a base, which also yields an equivalent of the conjugate acid (Scheme 4).^{39,40} Several factors are required for a successful reaction, such as the nature of the metal center, the base used, as well as the steric and electronic character of the diphosphine. Initial reports pointed towards nickel and platinum complexes as promising systems, while more recent studies have shown that rhodium complexes can also react successfully.^{41,42} Reaching the delicate balance between reactivity in the heterolytic cleavage of H₂ and the hydricity of the generated metal hydride has been an enormous challenge in this field and active research in several laboratories is currently underway to develop efficient hydride and proton transfer agents in a potential catalytic process.



M = Ni, Pt



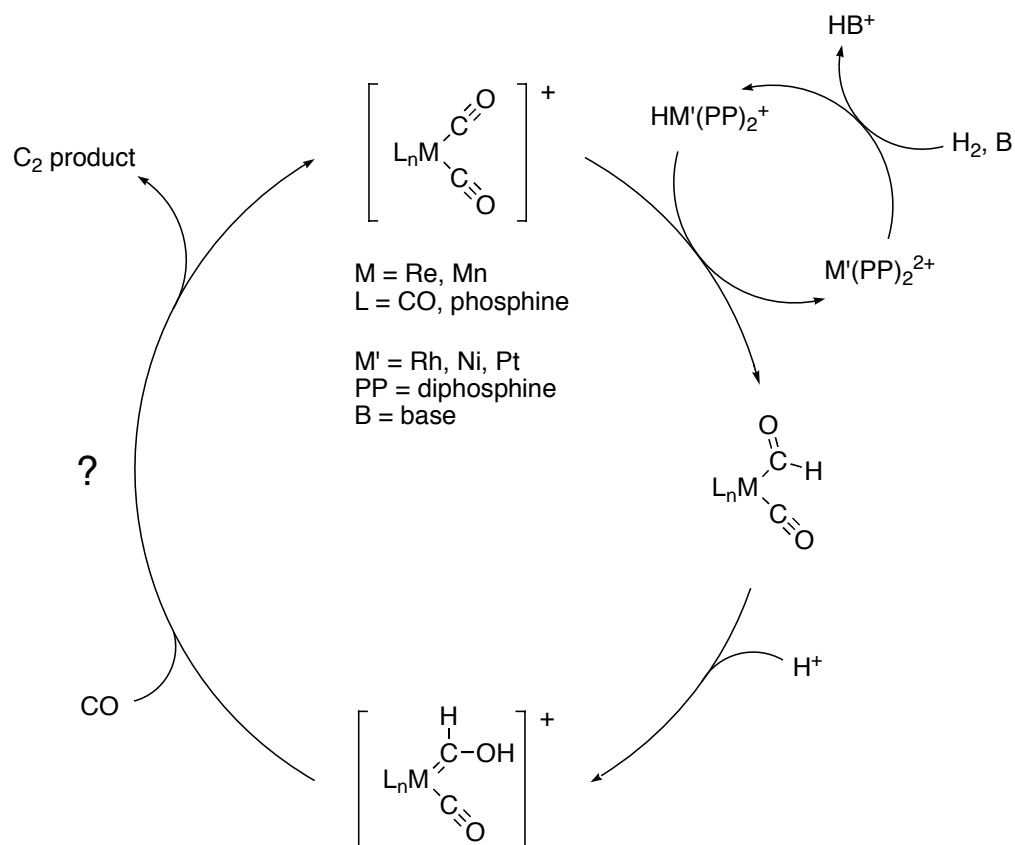
Scheme 4. Heterolytic cleavage of H₂.

Results and Discussion

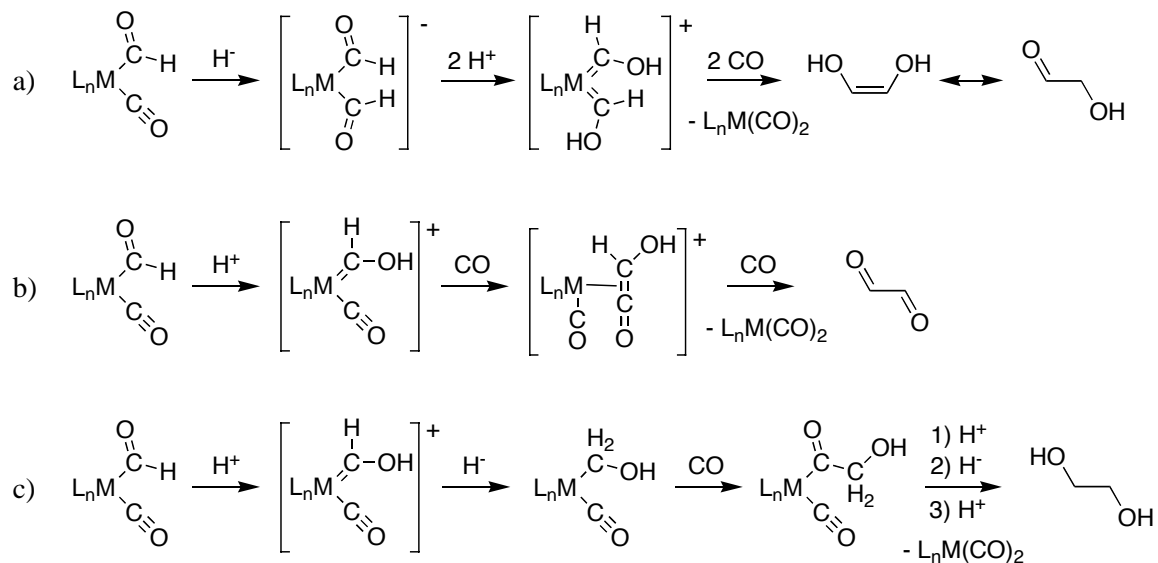
A Potential Idealized Catalytic Cycle

The present work has focused on demonstrating key steps useful in a potential catalytic cycle for the formation of ethylene glycol derivatives from synthesis gas. Along the way, important intermediates have been isolated and characterized. When devising such a catalytic system, two steps are particularly challenging and thus require special attention; firstly, the initial formation of a C-H bond, most likely as a formyl species and secondly, the formation of the C-C bond. With these considerations in mind and from the knowledge obtained from the extensive literature precedence, an idealized catalytic cycle

was designed (Scheme 5). An electrophilic transition metal carbonyl complex reacts with a suitable hydride source to generate the corresponding formyl species, as was described in the previous section. While this step is easily accomplished using main group hydrides such as LiHBEt_3 and NaBH_4 , a more desirable situation involves a carbonyl complex reactive enough to interact with a transition metal hydride, which in turn can be regenerated from H_2 , such as the DuBois systems discussed above.^{29,39-42} Treatment of the formyl species with an electrophile, such as a proton, generates a Fischer carbene. Closing the cycle and releasing the C_2 product can be envisioned *via* several pathways described in Scheme 6. Reaction of a second equivalent of hydride with the metal formyl species generates a diformyl intermediate, as has been demonstrated in a few examples (Scheme 3).^{26,33,34} Treatment with acid leads to the formation of a *bis*(carbene) species. C-C bond formation could be induced by the reaction with CO liberating glycolaldehyde (Scheme 6a). On the other hand, the hydroxycarbene intermediate could conceivably generate the corresponding hydroxyketene under CO pressure. Such transformations have been observed with Schrock-type carbenes.⁴³⁻⁴⁸ Releasing the organic fraction and tautomerization leads to glyoxal (Scheme 6b). Finally, another pathway involves the reduction of the hydroxycarbene by a hydride to the corresponding hydroxymethyl intermediate. Under CO pressure, migratory insertion leads to the formation of an acyl species. Generation of ethylene glycol is achieved by successive protonation and hydride reduction steps (Scheme 6c). Alternatively, reaction of the metal acyl with H_2 under certain conditions leads to glycolaldehyde, however releasing a metal hydride, which will require other transformations to be regenerated back to the metal carbonyl active species.



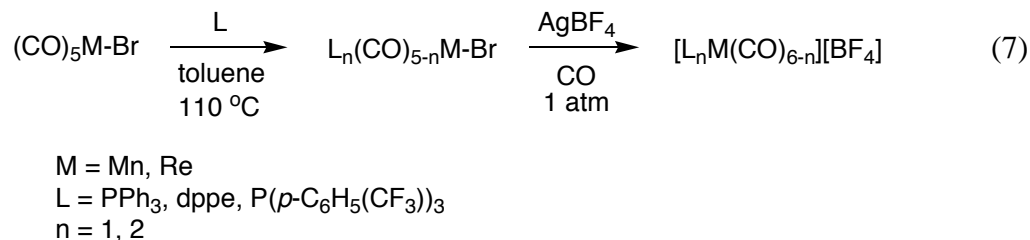
Scheme 5. Proposed idealized catalytic cycle for the synthesis of ethylene glycol derivatives from synthesis gas.



Scheme 6. Three possible pathways to the formation of C₂ products.

Preparation of Group 7 Carbonyl Complexes

A number of Group 7 carbonyl complexes were prepared. Inspired by reports from the Gibson laboratories,³⁵⁻³⁸ the general framework of complexes studied herein involves six-coordinate Group 7 carbonyl species supported by phosphine ligands. Their preparation is straightforward and requires initial synthesis of the phosphine-ligated metal bromide by simple ligand exchange followed by salt metathesis under an atmosphere of CO to generate the desired cationic carbonyl complexes (Eq. 7).



The complexes that were studied are presented in Figure 2 (**5-9**). Several issues are worth noting. Firstly, in all reactions involving salt metathesis with silver tetrafluoroborate, small amounts of silver salt impurities remained even after thorough purification. Due to their partial solubility in solvents such as CH₂Cl₂ and CH₃CN, repeated recrystallizations of the carbonyl complexes could not completely remove the silver impurities, which slowly darken the sample when not protected from light. Furthermore, while preparation of the bromide precursors of **5-8** was facile in toluene solutions at 110 °C for 15 hours, synthesis of the bromide precursor of **9** was much more difficult, as the total reaction time was over 10 days and required evacuating the liberated

CO to drive the reaction forward. Additionally, the solubility properties of **9** differ from that of the other complexes. While **5-8** are all quite soluble in CH₂Cl₂, **9** is not and workup was performed in CH₃CN.

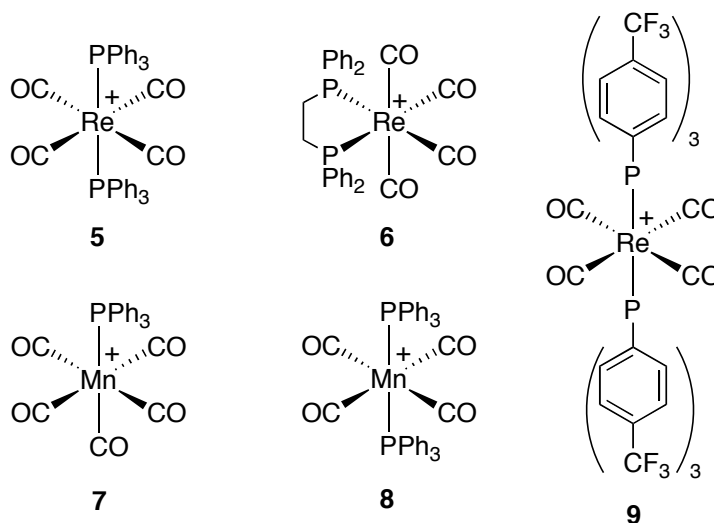


Figure 2. Group 7 carbonyl cations synthesized.

Synthesis of Group 7 Formyl Species

Carbonyl complex **5** ($\nu_{\text{CO}} = 2000 \text{ cm}^{-1}$) cleanly reacts with an equivalent of LiHBEt₃ in THF to generate the corresponding formyl species Re(PPh₃)₂(CO)₃(CHO) (**10**) in good yield. Addition of excess LiHBEt₃ does not generate the diformyl, presumably because the remaining carbonyl ligands are not electrophilic enough for a second hydride attack. Similarly, complex **5** does not react with transition metal hydrides such as [(dmpe)₂Pt(H)][PF₆]. Such metal hydrides are of course less hydridic than LiHBEt₃ and thus require more electrophilic metal carbonyls for reaction. To further highlight the need for electrophilic complexes, reactions with LiHBEt₃ were attempted

using analogous neutral chromium complexes. As expected, reaction of $\text{Cr}(\text{CO})_6$ ($\nu_{\text{CO}} = 2000 \text{ cm}^{-1}$) with LiHBEt_3 leads to a low conversion to the formyl complex $\text{Cr}(\text{CO})_5(\text{CHO})$ (ca. 35% by NMR). On the other hand, the more electron-rich $(\text{dppe})\text{Cr}(\text{CO})_4$ ($\nu_{\text{CO,avg}} = 1924 \text{ cm}^{-1}$) does not react with LiHBEt_3 , even when an excess of the hydride is present.

Formyl **10** is stable in solution for several hours, after which slow decomposition to a metal hydride occurs. This decomposition occurs by loss of a ligand (CO or phosphine) followed by hydride attack (the formyl hydrogen has been suggested to be hydridic), or simply by a deinsertion pathway. In the case of **10**, preferential loss of a phosphine over a CO ligand is observed to give $\text{HRe}(\text{PPh}_3)(\text{CO})_4$. This is evident in the ^1H NMR, which shows a doublet at -4.99 ppm corresponding to coupling to one phosphine. In order to slow down the decomposition process, $[(\text{dppe})\text{Re}(\text{CO})_4][\text{BF}_4]$ (**6**) was prepared. This complex is interesting not only because it could lead to a more stable formyl species, but also because the geometry around the metal center is altered; a diphosphine forces a *cis* geometry around the metal, while in the case of **5**, the two PPh_3 are arranged in a *trans* fashion. Reaction of **6** ($\nu_{\text{CO,avg}} = 2042 \text{ cm}^{-1}$) with LiHBEt_3 led to the formation of the desired formyl species in good yield. However, as would be expected when a *cis* complex is involved, both meridional and facial isomers of $(\text{dppe})\text{Re}(\text{CO})_3(\text{CHO})$ were observed in the ^1H NMR spectrum (Figure 3). The ^1H NMR spectrum shows strong preference for the formation of the *fac* isomer (> 9 : 1 ratio with *mer* isomer). Additionally, the spectrum clearly displays a difference in coupling constants whether the formyl group is *cis* or *trans* to the phosphines. In the case of the *fac* isomer where the formyl moiety is *cis* to both phosphorous centers, the coupling constant

is small (3.7 Hz), while the *mer* product exhibits a much larger coupling constant of 10.9 Hz, which corresponds to the formyl proton coupling to the *trans* phosphorous, with coupling to the *cis* phosphorous too small to be determined (Figure 3). While the formyl product is in fact more stable than **10**, it will eventually decompose giving predominantly $\text{HRe}(\text{dppe})(\text{CO})_3$, suggesting preferred loss of a CO ligand.

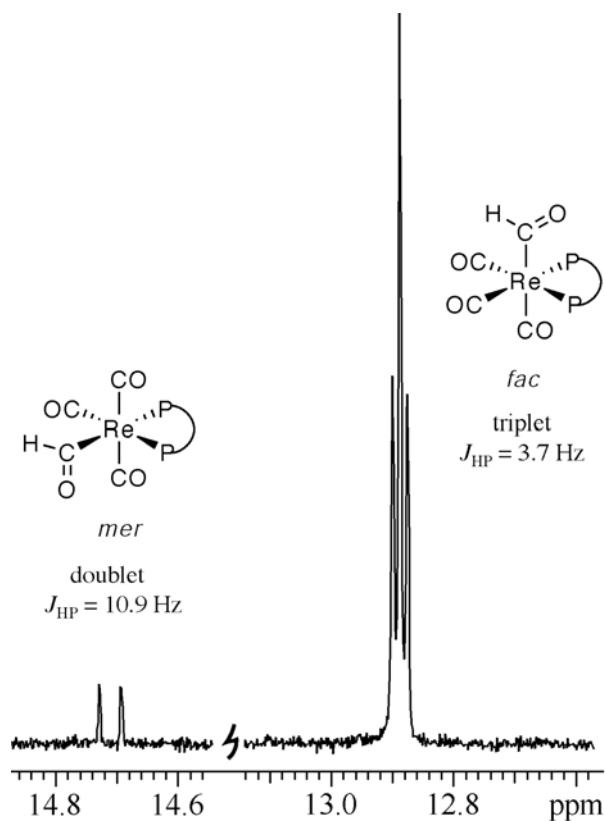


Figure 3. Formyl region of the ^1H NMR spectrum from the reaction of **6** with LiHBEt_3 depicting the two isomers *mer* (14.7 ppm) and *fac* (12.9 ppm) in a ratio of *ca.* 1: 9.

Manganese complex **8** behaved similarly to its rhenium analog **5** when reacted with LiHBEt_3 . The formyl product $\text{Mn}(\text{PPh}_3)_2(\text{CO})_3(\text{CHO})$ (**11**) was obtained cleanly with the diagnostic formyl signal appearing at 13.55 ppm in the ^1H NMR spectrum as a triplet from coupling to the two phosphine ligands ($J_{\text{HP}} = 2.0 \text{ Hz}$). This is in contrast to

the ^1H NMR spectrum of **10**, which only shows a singlet for the formyl signal due to the very small coupling to the phosphines. The decomposition pathway of **11** is in line with its rhenium analog with preferential loss of phosphine, leading to a hydride peak in the ^1H NMR spectrum as a doublet.

Reducing complex **7** to the corresponding formyl species is much less straightforward due to the instability of the formyl product $\text{Mn}(\text{PPh}_3)(\text{CO})_4(\text{CHO})$ (**12**). Because the carbonyl precursor **7** is so electrophilic ($\nu_{\text{CO,avg}} = 2086 \text{ cm}^{-1}$), the generated formyl is highly reactive and hydride attack occurs rapidly, leading to the formation of the corresponding hydride $\text{HMn}(\text{PPh}_3)(\text{CO})_4$ (**13**). When the reaction is performed at room temperature and is exposed to light, the product distribution immediately upon mixing is composed of **12** and **13** in a ratio of 3 : 7, respectively (Figure 4a). However when the reaction is carried out in a cold well inside the glovebox and kept at -78°C until NMR data acquisition, the ratio of products is improved to 10.5 : 1 : 3 for *cis*-**12**, *trans*-**12** and **13**, respectively (Figure 4b). Since the major decomposition pathway of the formyl species involves loss of CO, the reaction was also performed under an atmosphere of CO at room temperature upon mixing. In this case, the decomposition was moderately slowed down, as *cis*-**12**, *trans*-**12** and **13** appeared in ratios of 14 : 1 : 7, respectively (Figure 4c). Finally, a most surprising result occurred when $[(\text{dmpe})_2\text{Pt}(\text{H})][\text{PF}_6]$ was employed as the hydride source. Unlike complex **8**, which contains two phosphine ligands, carbonyl complex **7** is electron-deficient enough to react with transition metal hydrides. In a reaction carried out at room temperature with no added CO, $[(\text{dmpe})_2\text{Pt}(\text{H})][\text{PF}_6]$ reduced **7** to give a distribution of *cis*-**12**, *trans*-**12** and **13** in ratios of 11 : 1.5 : 1, respectively, as well as other minor unidentified decomposition products

(Figure 4d). After 2.5 hours, the ^1H NMR spectrum shows a product distribution of 7 : 1 : 3.5, further suggesting that the formyl complexes decompose over time to the hydride *via* loss of CO. While this system was not investigated further, the results presented here are very promising, because unlike **5**, **6** and **8**, complex **7** can be reduced by transition metal hydrides, which in turn are regenerated with H_2 . This element is crucial in designing catalysts capable of converting synthesis gas to valuable chemicals.

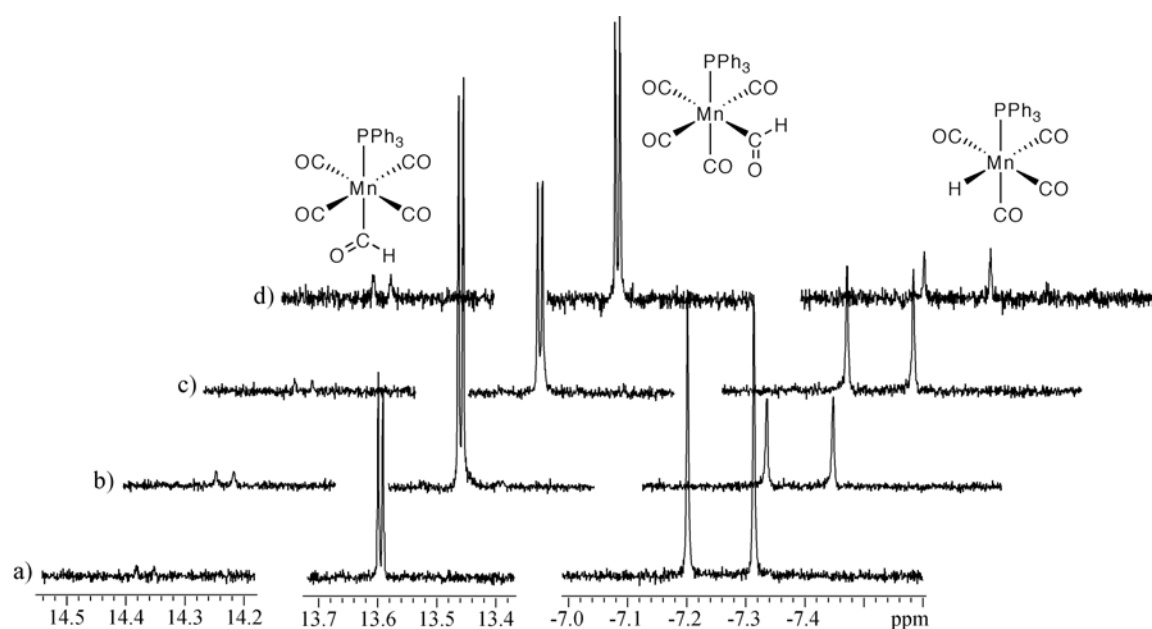
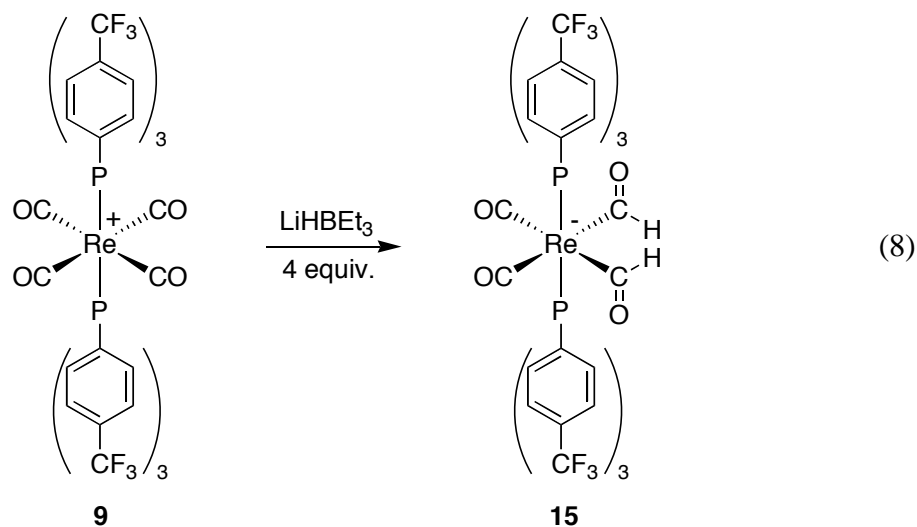


Figure 4. Reaction of complex **7** with hydride sources: a) LiHBEt_3 at room temperature. b) LiHBEt_3 at -78°C . c) LiHBEt_3 under 1 atm CO at room temperature. d) $[(\text{dmpe})_2\text{Pt}(\text{H})][\text{PF}_6]$ at room temperature.

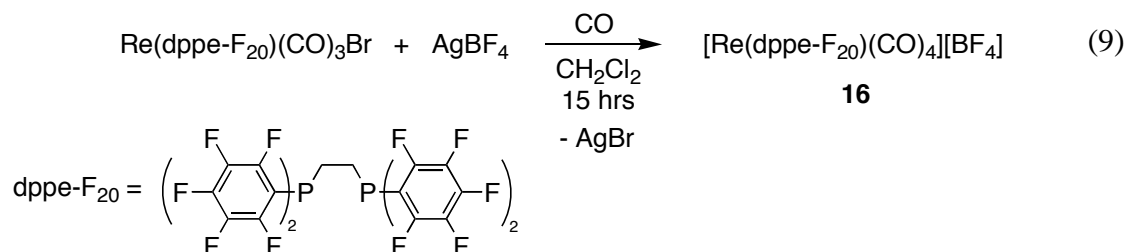
In an attempt to enhance the electrophilicity of complex **5**, CF_3 functionalities were strategically placed on the *para* position of the phenyl groups on the phosphines. The IR spectrum of complex **9** shows one stretch for the CO ligands at 2017 cm^{-1} , demonstrating the effect of the electron-withdrawing groups on the phosphines. When **9** is allowed to react with an equivalent of LiHBEt_3 , the corresponding formyl species **14** is

generated with a diagnostic peak at 16.8 ppm in the ^1H NMR spectrum. Adding two equivalents of the hydride to **9** leads to the formation of two products, which are identified as **14** and the diformyl species $\text{Re}(\text{P}(\text{C}_6\text{H}_4(p\text{-CF}_3))_3)_2(\text{CO})_2(\text{CHO})_2$ (**15**). When four equivalents of LiHBEt_3 are added to complex **9** however, only diformyl product **15** is observed by NMR (Eq. 8). This result is in sharp contrast with experiments run using **5**, which was determined not to be electrophilic enough to allow two successive reductions to generate a diformyl species. While this new complex was not investigated further, it represents a new example in a class of compounds that has been quite uncommon, as was discussed in the introduction. Furthermore, this compound allows the investigation of potential *bis*(carbene) species and subsequent coupling reactions.



In yet another attempt at preparing electron-deficient metal carbonyl complexes, complex **16** was synthesized. Analogous to compound **6**, carbonyl complex **16** is composed of a *bis*-diphenylphosphinoethane-type ligand, where all aryl positions have been fluorinated. It is synthesized from the corresponding bromide $\text{Re}(\text{dppe-F}_{20})(\text{CO})_3\text{Br}$

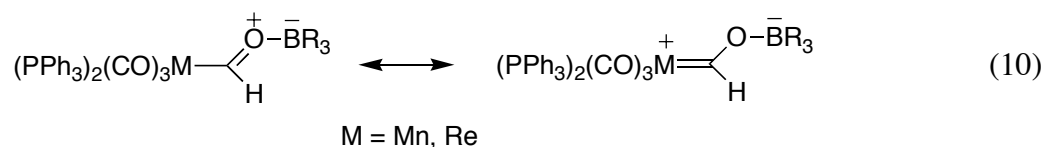
in a manner similar to other analogs discussed earlier by salt metathesis using AgBF_4 under an atmosphere of CO (Eq. 9). Unfortunately, attempts at reducing the carbonyl complex in the presence of a hydride source such as LiHBEt_3 were thwarted by a nucleophilic aromatic substitution side-reaction. This compound was not investigated further.

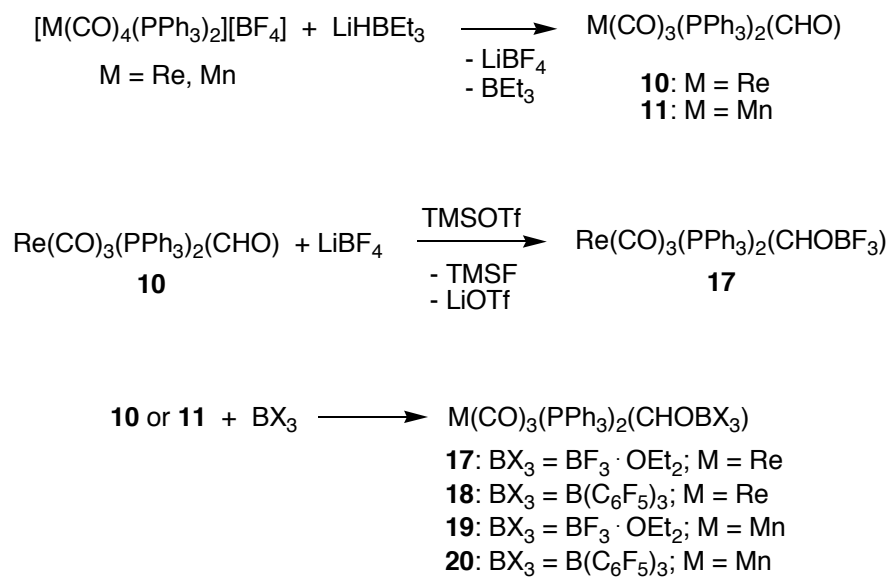


Synthesis and Reactivity of Borane-Stabilized Group 7 Formyl Complexes

In hopes of preparing cationic rhenium(I) Fischer carbenes from the corresponding rhenium formyl complex $\text{Re}(\text{PPh}_3)_2(\text{CO})_3(\text{CHO})$ (**10**), and in particular a reactive siloxycarbene species, a novel type of neutral borane-stabilized rhenium formyl was isolated. Addition of a CH_2Cl_2 solution of TMS^+OTf^- ($\text{TMS} = \text{Si}(\text{CH}_3)_3$; $\text{OTf} = \text{CF}_3\text{SO}_3$) to **10**, prepared *in situ* from $[\text{Re}(\text{PPh}_3)_2(\text{CO})_4][\text{BF}_4]$ (**5**) and LiHBEt_3 (see above), generated after work up and recrystallization from CH_2Cl_2 / petroleum ether $\text{Re}(\text{PPh}_3)_2(\text{CO})_3(\text{CHOBF}_3)$ (**17**) in good yield (Scheme 7). The unexpected product formation can be rationalized by the abstraction of a fluoride from the LiBF_4 byproduct by TMS^+ releasing TMSF and BF_3 , which then binds the formyl oxygen. Complex **17**, which can be prepared in almost quantitative yield by reacting formyl **10** directly with $\text{BF}_3 \cdot \text{OEt}_2$, was fully characterized including an X-ray structure determination (Figure 5).

The bond lengths for Re-C4 (2.096(3) Å) and C4-O4 (1.270(4) Å) may be compared to those of the cationic rhenium methoxy carbene $[\text{Re}(\text{CO})_3(\text{PPh}_3)_2(\text{CHOCH}_3)][\text{OTf}]$ (2.064(3) and 1.290(4) Å, respectively; see next section), as well as its manganese analog $[\text{Mn}(\text{CO})_3(\text{PPh}_3)_2(\text{CHOCH}_3)][\text{OTf}]$ first prepared by Gibson and coworkers (C-O: 1.286 Å),³⁶ the neutral formyl complex $\text{Re}(\text{C}_5\text{Me}_5)(\text{NO})(\text{PPh}_3)(\text{CHO})$ (2.055 and 1.221 Å, respectively),⁴⁹ and typical Re-C bond lengths (2.24-2.32 Å).⁵⁰⁻⁵² These values suggest that the nature of the interaction between rhenium and carbon lies somewhere between a carbene $\text{Re}=\text{C}$ bond,⁵³⁻⁵⁶ and a formyl Re-C bond, so that complex **17** can be described either as a borane-stabilized formyl or a boroxycarbene complex (Eq. 10). Interestingly, **17** represents the first example of such a complex, and is particularly significant because coordination of a Lewis acid to oxygen is a common strategy for activation towards further reduction and/or C-C bond formation by insertion.





Scheme 7. Preparation of rhenium and manganese boroxycarbene complexes **17-20**.

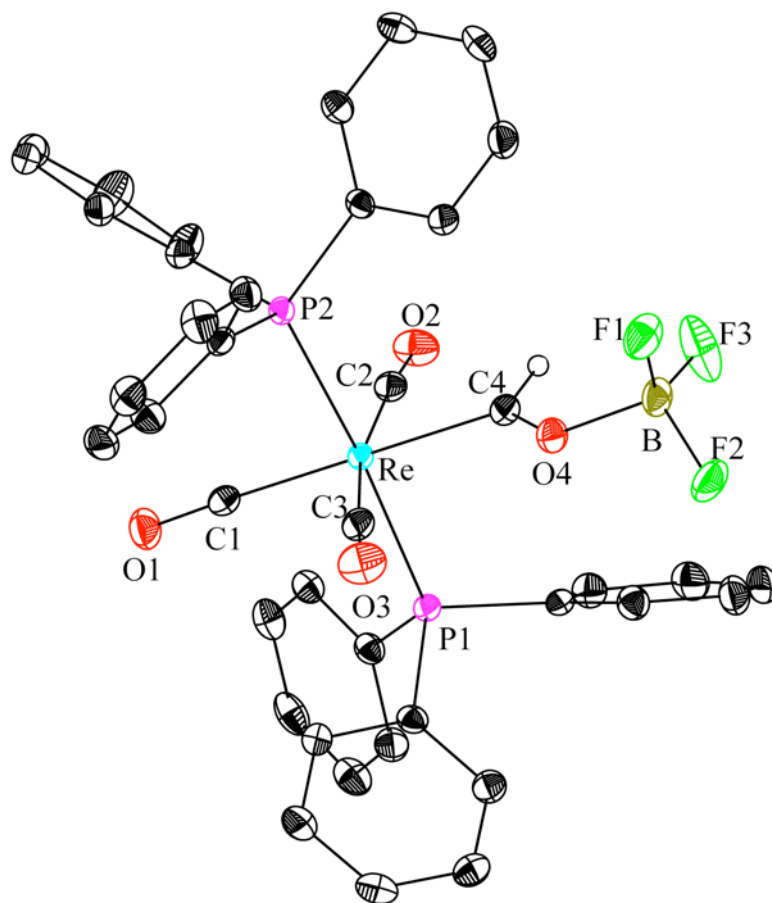


Figure 5. Structural drawing of **17** with thermal ellipsoids at the 50% probability level. Selected bond lengths (Å) and angles (°): Re-C4, 2.096(3); Re-CO (avg), 1.980; C4-O4, 1.270(4); O4-B, 1.544(4); Re-C4-O4, 125.8(2); C4-O4-B, 124.6(3).

As was discussed earlier, formyl complexes are typically quite labile in solution, often decomposing irreversibly to the corresponding carbonyl hydride species with concomitant loss of a ligand. In contrast, **17** is surprisingly unreactive, both in solution and in the solid state. Exposing the carbene complex to PMe_3 at 40 °C, or to 1-10 atm CO, for several days, in attempts to induce C-C bond formation, resulted in virtually no detectable reaction (less than 1% of free PPh_3 was observed).

Use of $\text{B}(\text{C}_6\text{F}_5)_3$ as the stabilizing borane gave the analogous carbene species **18**, with a very similar X-ray structure (Figure 6); the same methods afforded the

corresponding manganese complexes $\text{Mn}(\text{PPh}_3)_2(\text{CO})_3(\text{CHOBf}_3)$ (**19**) and $\text{Mn}(\text{PPh}_3)_2(\text{CO})_3(\text{CHOB}(\text{C}_6\text{F}_5)_3)$ (**20**) (Scheme 7). While the stability of **19** appears to be similar to that of its rhenium analog **17**, complex **20** decomposes at room temperature to form a borohydride salt of the parent cationic carbonyl, $[\text{Mn}(\text{CO})_4(\text{PPh}_3)_2][(\text{C}_6\text{F}_5)_3\text{BH}]$, **21** (Scheme 8). Nevertheless, we were able to obtain an X-ray structure of **20** (Figure 7); its geometry is closely similar to that of **18**.

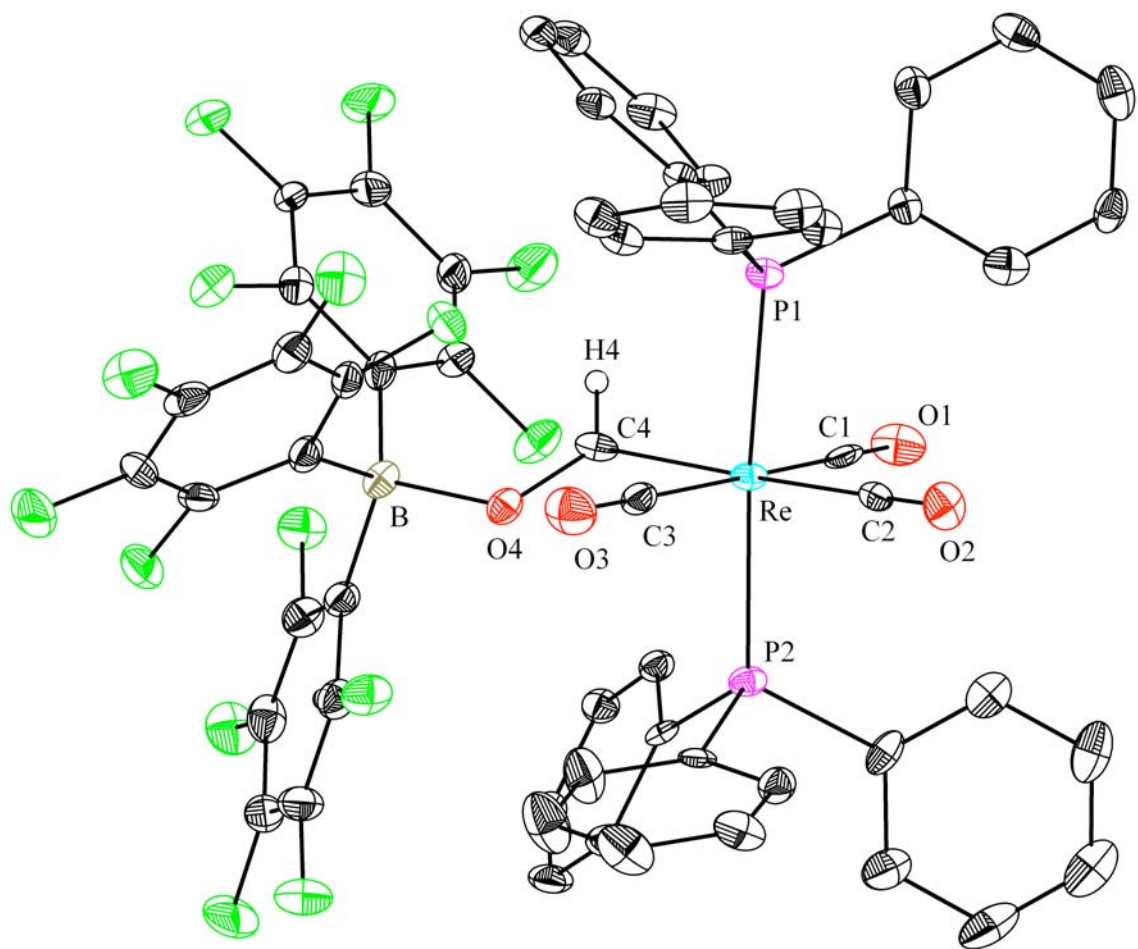


Figure 6. Structural drawing of **18** with thermal ellipsoids at the 50% probability level. Selected bond lengths (Å) and angles (°): Re-C4, 2.125(5); Re-CO (avg), 1.980; C4-O4, 1.282 (5); O4-B, 1.575(6); Re-C4-O4, 126.9(3); C4-O4-B, 130.6(4).

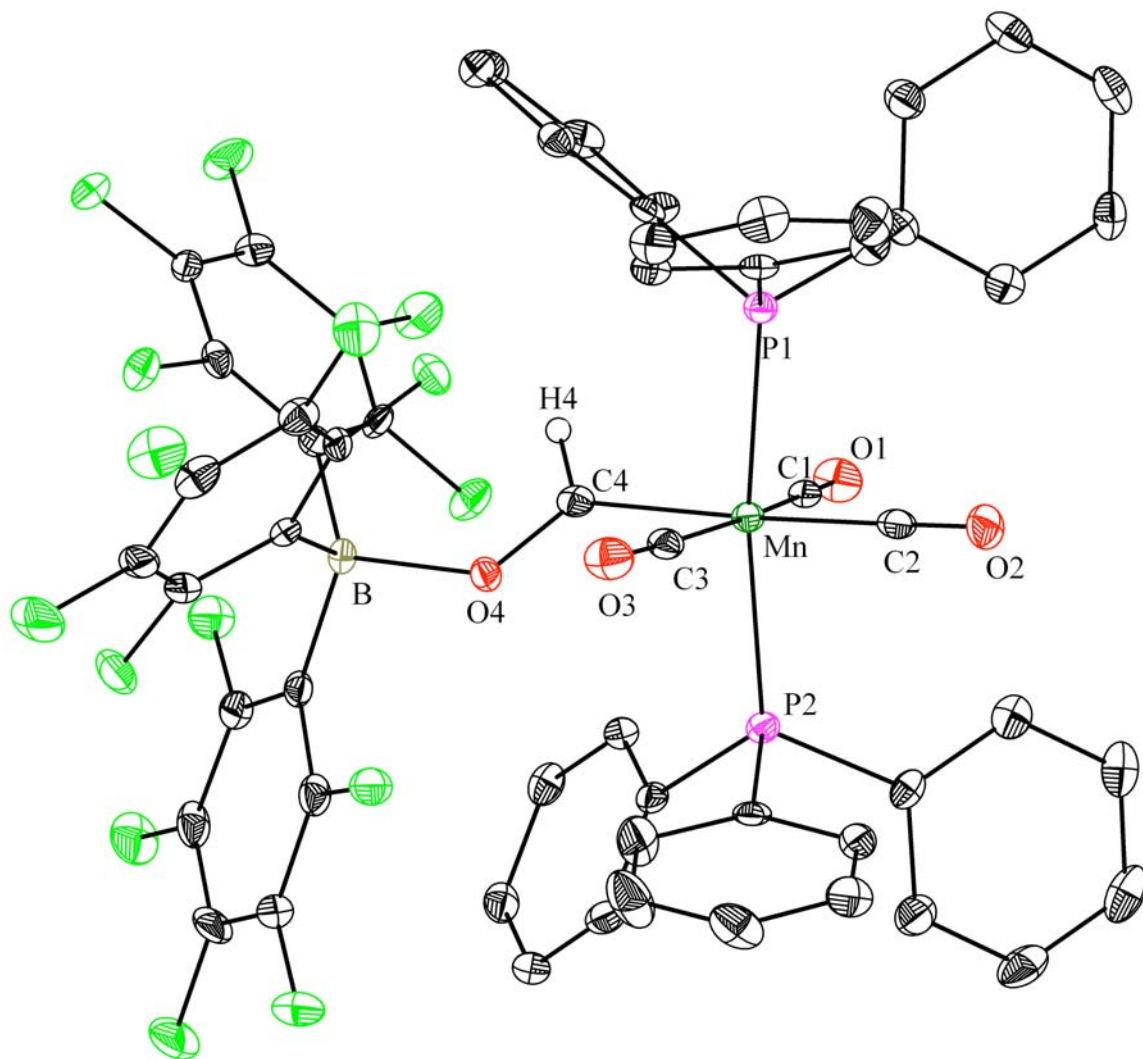


Figure 7. Structural drawing of **20** with thermal ellipsoids at the 50% probability level. Selected bond lengths (Å) and angles (°): Mn-C4, 1.994(2); Mn-CO (avg), 1.8₃₉; C4-O4, 1.275(2); O4-B, 1.593(3); Mn-C4-O4, 127.40(16); C4-O4-B, 129.96(17).

It thus appears that the relative hydricity of the manganese formyl compared to that of the borohydride $[(\text{C}_6\text{F}_5)_3\text{B-H}]^-$ favors the latter in this case, hampering isolation of **20** as a stable, pure product; in the absence of light, irreversible decomposition of **20** to **21** is the only pathway observed by NMR spectroscopy, following clean first-order kinetics (Figure 8). It seems reasonable to suggest that $\text{B}(\text{C}_6\text{F}_5)_3$ first dissociates from **20** in solution, releasing **11** which then delivers its hydride to the borane, although no

evidence for the presence of “naked” formyl **11** was observed. When the sample was exposed to light, the carbene peaks disappeared and new peaks for manganese hydride **13** grew, along with formation of a phosphine-borane adduct. It is unlikely that **13** is generated directly from **21**. One scenario for formation of **13** might be reversible loss of a phosphine ligand from the cationic manganese carbonyl complex **21** to generate a coordinatively unsaturated species, followed by hydride transfer to form **13** and the phosphine-borane adduct; however, the reaction of $[\text{Mn}(\text{CO})_4(\text{PPh}_3)_2][\text{BF}_4]$ with LiHBEt_3 does not immediately generate **13**, as would be expected if this route were operational. Furthermore, exposing a 4:1 mixture of **21** and **20** to light generated a 4:1 mixture of **21** and **13**, respectively, indicating that **13** arises directly from **20**, not **21** (Scheme 8). The requirement of light to induce formation of the hydride suggests possible involvement of radical pathways, as is known to occur in similar systems.^{57,58} The instability of complex **20** is in sharp contrast with that of **18**, as the latter can be isolated in pure form and shows no signs of decomposition or $\text{B}(\text{C}_6\text{F}_5)_3$ dissociation after 24 hours in solution at room temperature.

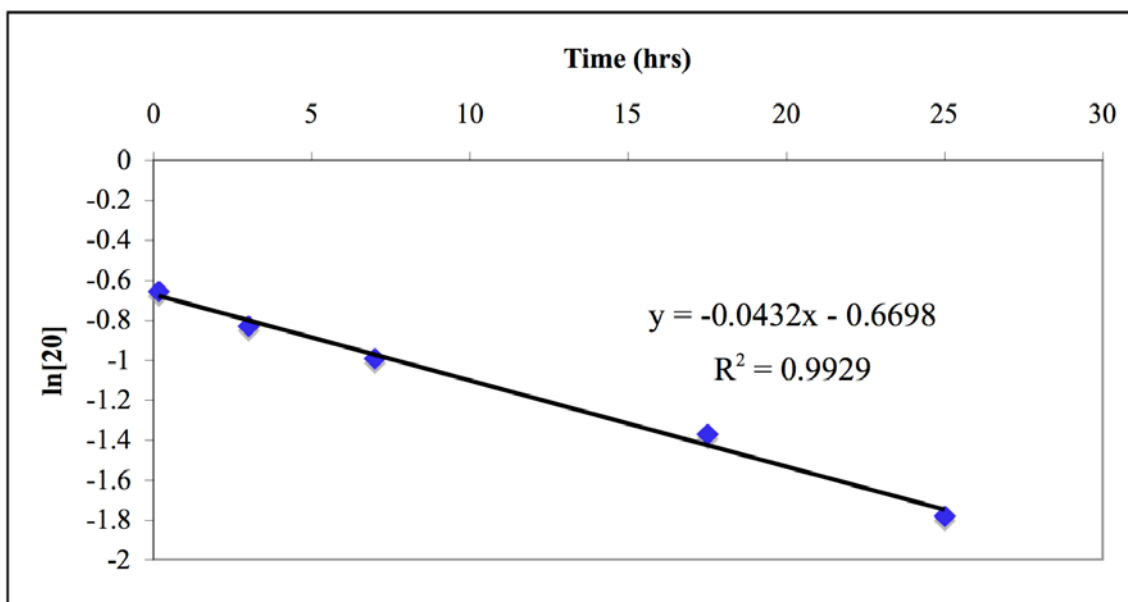
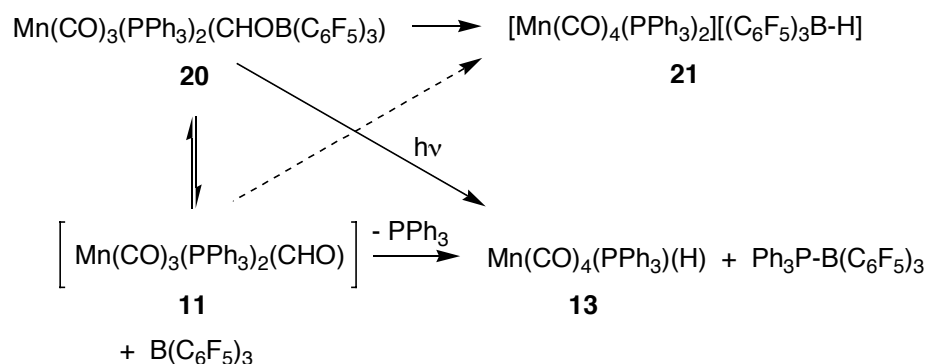


Figure 8. Disappearance of **20** over time indicates first-order decomposition.



Scheme 8. Proposed decomposition pathway of **20** into complex **21** and manganese hydride **13**.

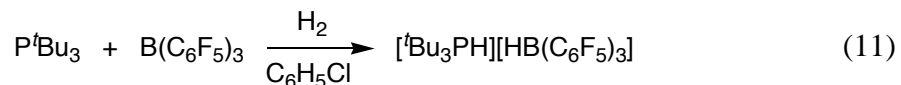
We were interested in using **17** as a synthon for the preparation of various cationic carbene species. The surprising stability of the complex was further demonstrated when **17** was allowed to react with CH_3OTf for several days at room temperature in CH_2Cl_2 . No transformation to the corresponding cationic methoxycarbene was observed. Increasing the temperature to 40°C and allowing the reaction to run overnight led to

partial formation of the desired $[\text{Re}(\text{CO})_3(\text{PPh}_3)_2(\text{CHOMe})][\text{OTf}]$ (10% conv. by ^1H NMR; 17% after 2 days). Conversion was increased to 20% when an excess of Et_2O was added at room temperature to promote the formation of the $\text{BF}_3\cdot\text{OEt}_2$ adduct. It was anticipated that the weaker interaction of the less Lewis acidic $\text{B}(\text{C}_6\text{F}_5)_3$ with the formyl in **18** would allow the formation of the methoxycarbene to go to completion, however slow conversion to CH_4 and $[\text{Re}(\text{CO})_4(\text{PPh}_3)_2][\text{OTf}]$ as well as minor unidentified products was observed instead, further highlighting the hydricity of the formyl hydrogen. Despite the stability differences between **18** and **20**, their reactivity showed similarities, as treating the manganese analog **20** with CH_3OTf resulted in the same products, with no sign of the cationic carbene species. It is not yet clear whether CH_4 is formed from the $[(\text{C}_6\text{F}_5)_3\text{B-H}]^-$ species or directly from the formyl-borane adduct.

Furthermore, reacting **17** or **19** with a hydride source, such as LiHBEt_3 or NaHBEt_3 , led to the partial formation of formyls **10** and **11**, respectively as well as H-BF_3^- . Generation of a boroxymethyl species, corresponding to hydride attack on the carbene carbon was not observed. This is in sharp contrast with recent findings in our laboratories, whereby the reaction of NaHBEt_3 with a rhenium formyl species stabilized intramolecularly, by an alkylborane tethered to the phosphine ligand, leads to the formation of the corresponding boroxymethyl species, which then proceeds to undergo CO insertion to form a C-C bond.⁵⁹

Finally, complexes **18** and **20** were particularly interesting in their role in potential transformations relevant to synthesis gas conversion. Stephan and coworkers have recently reported the facile heterolytic cleavage of H_2 by phosphines and boranes (Eq. 11).⁶⁰ We explored the possibility of using the phosphonium borohydride product as a

hydride and proton transfer agent to the manganese formyl to form the corresponding hydroxymethyl species. However, reaction of **18** with the preformed [^tBu₃P-H][(C₆F₅)₃B-H] in chlorobenzene did not result in any reaction at room temperature over 2 days. Raising the temperature to 45 °C overnight lead to the decomposition of **18** to [Re(CO)₄(PPh₃)₂][(C₆F₅)₃B-H], presumably *via* a similar pathway as discussed in Scheme 8, without involvement of the phosphonium borohydride. Direct reaction of **18** with P^tBu₃ under 3.5 atm of H₂ did not lead to products after several hours at room temperature either. No evidence for the formation of the phosphonium borohydride species was observed, presumably because B(C₆F₅)₃ does not dissociate from the formyl. Heating the solution to 45 °C for 10 hours led to the partial decomposition of **18** to [Re(CO)₄(PPh₃)₂][(C₆F₅)₃B-H]. On the other hand, a room temperature reaction comprised of **20** and P^tBu₃ under 3.5 atm of H₂ led to a partial conversion to formyl **11** suggesting B(C₆F₅)₃ dissociation, however there was no evidence for the formation of the phosphonium borohydride or further reaction thereof, despite the presence of small amounts of B(C₆F₅)₃. A control reaction showed that formyl **11** is also liberated without added H₂. Over time, **11** is slowly converted to the manganese hydride.

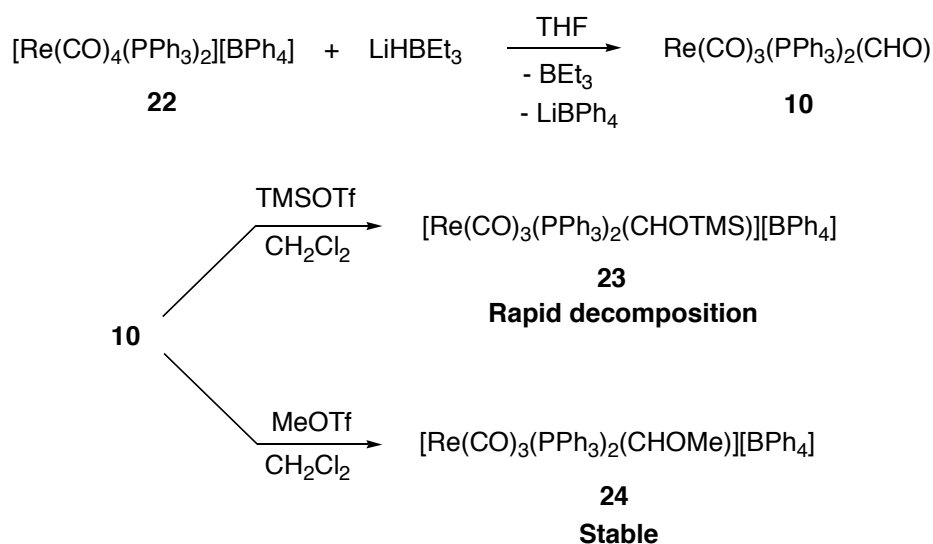


Synthesis of Cationic Group 7 Fischer Carbenes

As was mentioned in the previous section, the preparation of siloxycarbene complexes was hampered by the side-reaction occurring between the LiBF₄ byproduct

and TMSOTf. Therefore, an alternate carbonyl precursor was synthesized, which did not possess a reactive BF_4^- anion. Synthesis of $[\text{Re}(\text{PPh}_3)_2(\text{CO})_4][\text{B}(\text{C}_6\text{H}_5)_4]$ (**22**) is quite straightforward. A CH_2Cl_2 solution containing **5** and $\text{Na}[\text{B}(\text{C}_6\text{H}_5)_4]$ was allowed to react for three days. After removing the insoluble impurities by filtration and the solvent *in vacuo*, the resulting product was recrystallized from CH_2Cl_2 /petroleum ether to give **22** in excellent yield.

A cationic rhenium siloxycarbene complex was prepared by the reaction of **10**, preformed *in situ* using **22**, with TMSOTf in CD_2Cl_2 following typical procedures. The newly formed carbene species, $[\text{Re}(\text{PPh}_3)_2(\text{CO})_3(\text{CHOTMS})][\text{B}(\text{C}_6\text{H}_5)_4]$ (**23**), shows a diagnostic carbene peak in the ^1H NMR spectrum at 13.91 ppm, while one singlet is present in the ^{31}P NMR spectrum at 11.3 ppm. Surprisingly, complex **23** decomposes rapidly when warmed to room temperature to the carbonyl precursor **22** releasing trimethylsilane (Scheme 9), and could therefore not be isolated in a pure form. The reason for such instability is not yet clear. Reactivity studies on complex **23** were very limited due to its rapid decomposition and all reactions attempted in order to induce C-C bond formation were unsuccessful. This complex was not investigated further.



Scheme 9. Synthesis of cationic rhenium Fischer carbene complexes **23** and **24**.

On the other hand, reacting formyl species **10** with methyl triflate under similar conditions cleanly generates the desired methoxycarbene complex $[\text{Re}(\text{PPh}_3)_2(\text{CO})_3(\text{CHOCH}_3)][\text{B}(\text{C}_6\text{H}_5)_4]$ (**24**) in very good yield (Scheme 9). In contrast to the siloxycarbene discussed above, the methoxy carbene product is stable in solution and pure samples can be isolated in the solid state, for which an X-ray structure determination was obtained (Figure 9). While the ^{31}P NMR spectrum shows a sharp singlet at 11.6 ppm, the diagnostic carbene peak in the ^1H NMR spectrum is observed at 11.94 ppm, significantly upfield when compared to its siloxycarbene analog **23**.

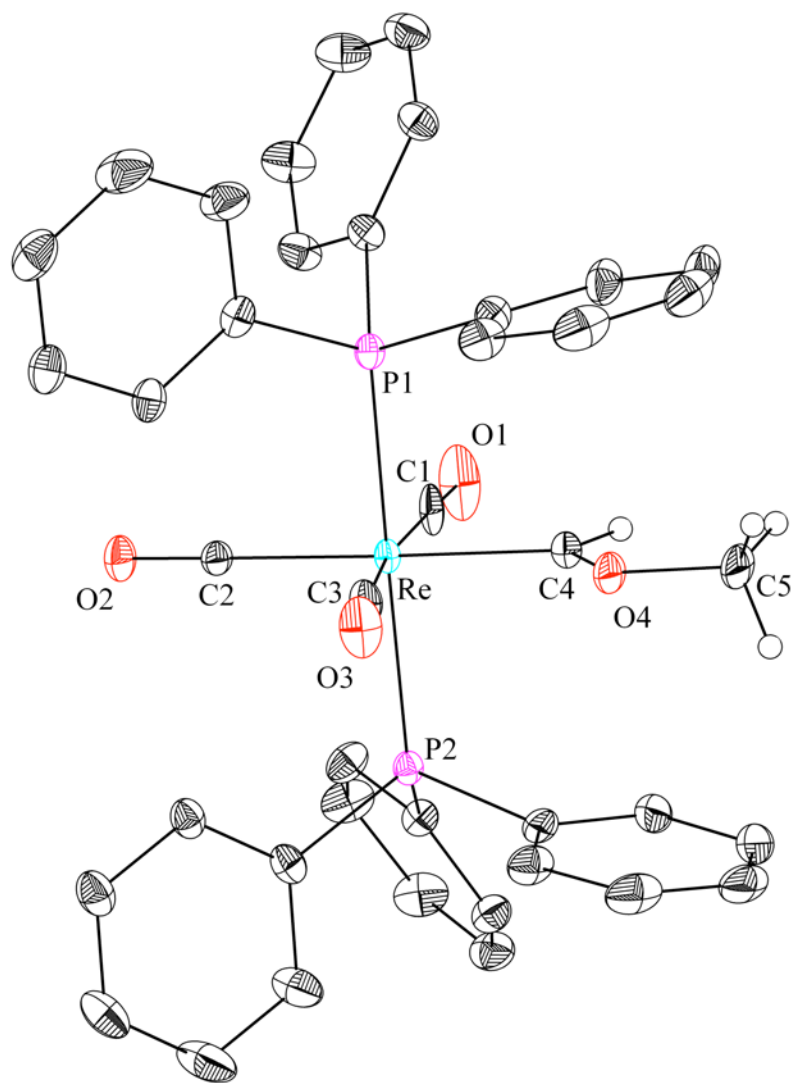
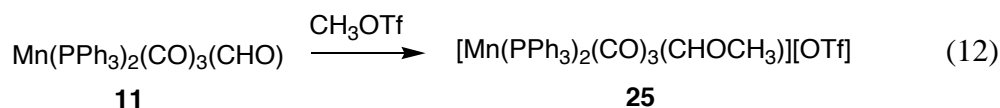
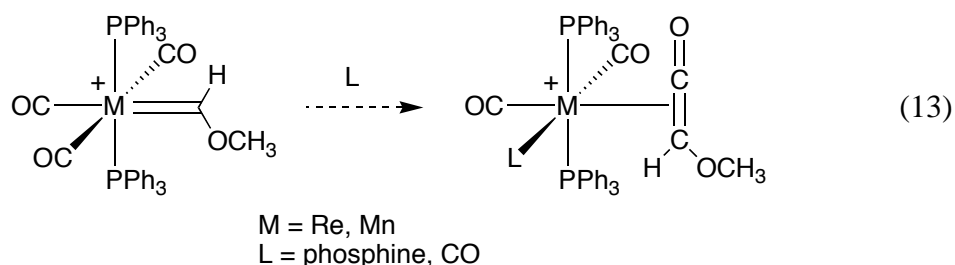


Figure 9. Structural drawing of **24** with thermal ellipsoids at the 50% probability level. Selected bond lengths (Å) and angles (°): Re-C4, 2.064(3); Re-CO (avg), 1.992; C4-O4, 1.290(4); O4-C5, 1.459(4); Re-C4-O4, 123.83(19); C4-O4-C5, 120.40(24).

In a similar fashion, the manganese analog $[\text{Mn}(\text{PPh}_3)_2(\text{CO})_3(\text{CHOCH}_3)][\text{OTf}]$ (**25**) was prepared from the reaction of manganese formyl species **7** with CH_3OTf in CH_2Cl_2 (Eq. 12). Complex **25** was originally reported by Gibson and coworkers,³⁶ and an X-ray structure determination was obtained as was discussed in the previous section.



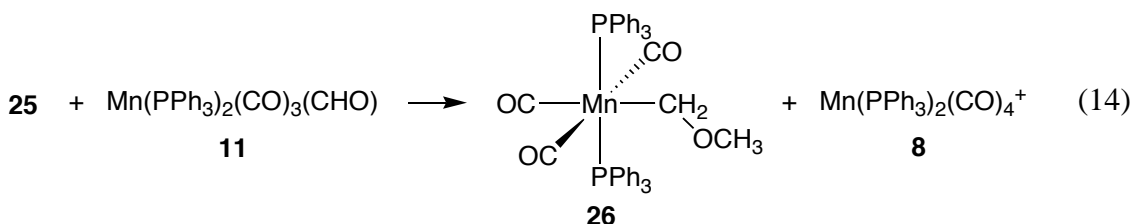
Methoxycarbene complexes **24** and **25** were used in reactivity studies in the hopes of demonstrating C-C bond forming reactions. By reacting the complexes with phosphines or placing them under high pressures of CO, the formation of methoxyketene species was targeted, as is depicted in Eq. 13. However, all attempts were found unsuccessful when PMe₃ was added to solutions of either **24** or **25**, and when such solutions were subjected to pressures of CO as high as 1000 psi. When a solution of **25** is allowed to stand for several days, the complex decomposes to an unidentified product. However, neither the nature of the decomposition product nor the rate of decomposition are affected when 1000 psi CO are added to a high-pressure NMR tube containing a solution of **25**.



Over the course of the last decade, Sierra and coworkers have studied the palladium-catalyzed transmetalation from Group 6 Fischer carbenes.^{61,62} While most examples seemed to target applications in organic synthesis, we have investigated the possibility of employing a similar strategy for the coupling of two Group 7 Fischer

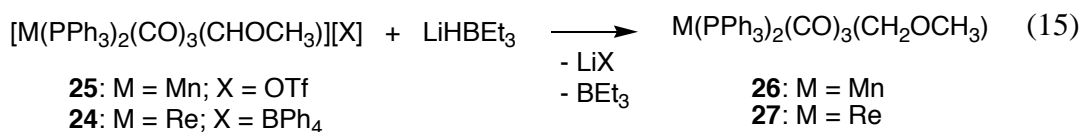
carbenes to generate an ethylene glycol derivative. Several experiments were run using complex **24** with either palladium(0) or palladium(II) sources, which were all found to be unsuccessful. When **24** is added to a THF-*d*₈ suspension containing 20 mol% Pd(OAc)₂ and NEt₃, a messy reaction occurs leading to the formation of many untraceable products, and after several hours, to the accumulation of Pd black. A control reaction confirmed that complex **24** is stable in the presence of NEt₃ for at least three hours. On the other hand, when Pd₂(dba)₃ (20 mol%) is used in CD₂Cl₂ instead, no reaction is observed in the ¹H NMR spectrum after 24 hours, despite a change in color when heated to 42 °C.

The methoxycarbene complexes are reactive to hydride attack. This was originally reported by Gibson and coworkers when **25** was allowed to react with its formyl analog **11** to generate a methoxymethyl species and an equivalent of the carbonyl cation **8** (Eq. 14).³⁷ In this case, the hydridic hydrogen from the formyl species delivers a hydride to the electrophilic carbene carbon on **25**. Of course other hydride sources also lead to successful reaction.



LiHBet₃ was used to reduce complexes **25** and **24** to their respective methoxymethyl species **26** and Re(PPh₃)₂(CO)₃(CH₂OCH₃) (**27**) (Eq. 15). One equivalent of the hydride source led almost immediately to the clean and quantitative conversion to the desired product. In both cases, the ¹H NMR spectra are diagnostic, as the downfield

carbene peaks disappear and new methylene signals grow as triplets at 3.60 ppm ($J_{\text{HP}} = 7.6$ Hz) and 3.22 ppm ($J_{\text{HP}} = 7.1$ Hz) for **26** and **27**, respectively. While **26** is stable in solution for extended periods of time, **27** eventually decomposes after several hours to unidentified products. Moreover, an X-ray structure determination of complex **26** was obtained (Figure 10). The general structural data seem to be in line with that of similar compounds. Nevertheless, while all analogous complexes exhibit a bending of the two *cis* CO ligands towards the alkyl moiety, the C1-Mn-C3 angle from **26** seems to be a little smaller than typically observed (160°).



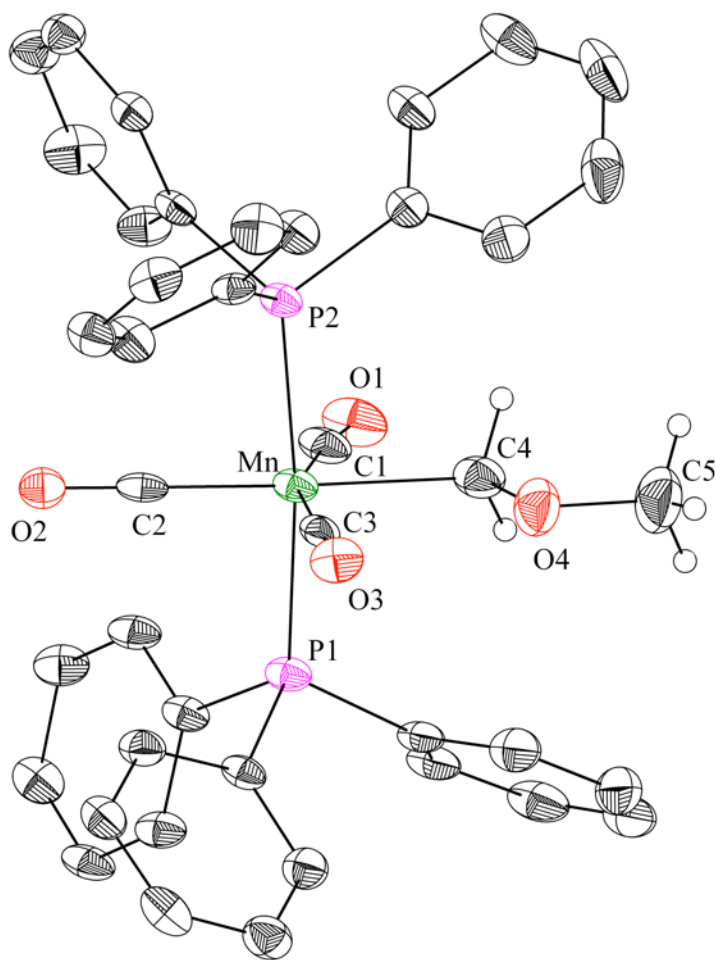


Figure 10. Structural drawing of **26** with thermal ellipsoids at the 50% probability level. Selected bond lengths (Å) and angles (°): Mn-C4, 2.156(3); Mn-CO (avg), 1.815; C4-O4, 1.455(3); C1-Mn-C3, 160.00(11); Mn-C4-O4, 113.35(16); C4-O4-C5, 111.2(2).

Reactivity of Manganese Methoxymethyl Species: Release of Dimethyl Ether and C-C Bond Formation *via* Migratory Insertion

Manganese methoxymethyl complex **26** displays very interesting reactivity. It was previously shown that both **26** and *cis*-Mn(PPh₃)(CO)₄(CH₂OCH₃) (**28**) generate the corresponding halomethyl complexes when treated with HX (X = Cl, Br, I).⁶³ During our investigation of the reactivity of **26**, we discovered that the methylene carbon acts as an electrophile in an S_N2-like reaction with a hydride source such as NaHBet₃ that leads to

the formation of dimethyl ether in moderate yield (*ca.* 60-75%, depending on the conditions) as well as minor unidentified products (Scheme 10). When a THF-*d*₈ solution of **26** was treated with one equivalent of NaHBET₃ in toluene, the slow reaction occurred over the course of several days, which was monitored by ¹H NMR spectroscopy (Figure 11). Not surprisingly, the rate of reaction is significantly increased when excess hydride is added to the solution. Initial attack of the hydride releases dimethyl ether and [Mn(PPh₃)₂(CO)₃]⁻, which likely undergoes further reaction with reactive impurities or borane present in solution (Scheme 10). It was established that neither Mn(PPh₃)₂(CO)₃(CH₃) nor CH₃Cl, which could arise from attack of the manganese anion on traces of CH₂Cl₂, followed by reaction with a second equivalent of hydride, are byproducts. After removing all volatiles on a high vacuum line and re-dissolving the remaining residue, only peaks corresponding to the minor unidentified byproducts were observed in the ¹H NMR spectrum, suggesting these are manganese species or other non-volatile byproducts. Interestingly, a similar reaction using the rhenium analog **27** did not lead to products. This is perhaps not surprising as it is expected that the rhenium anion would not be as good a leaving group as the manganese analog. To the best of our knowledge, this reaction represents the first example of this type of transformation on manganese alkyls and could play an important role in potential catalytic processes involving CO reduction.

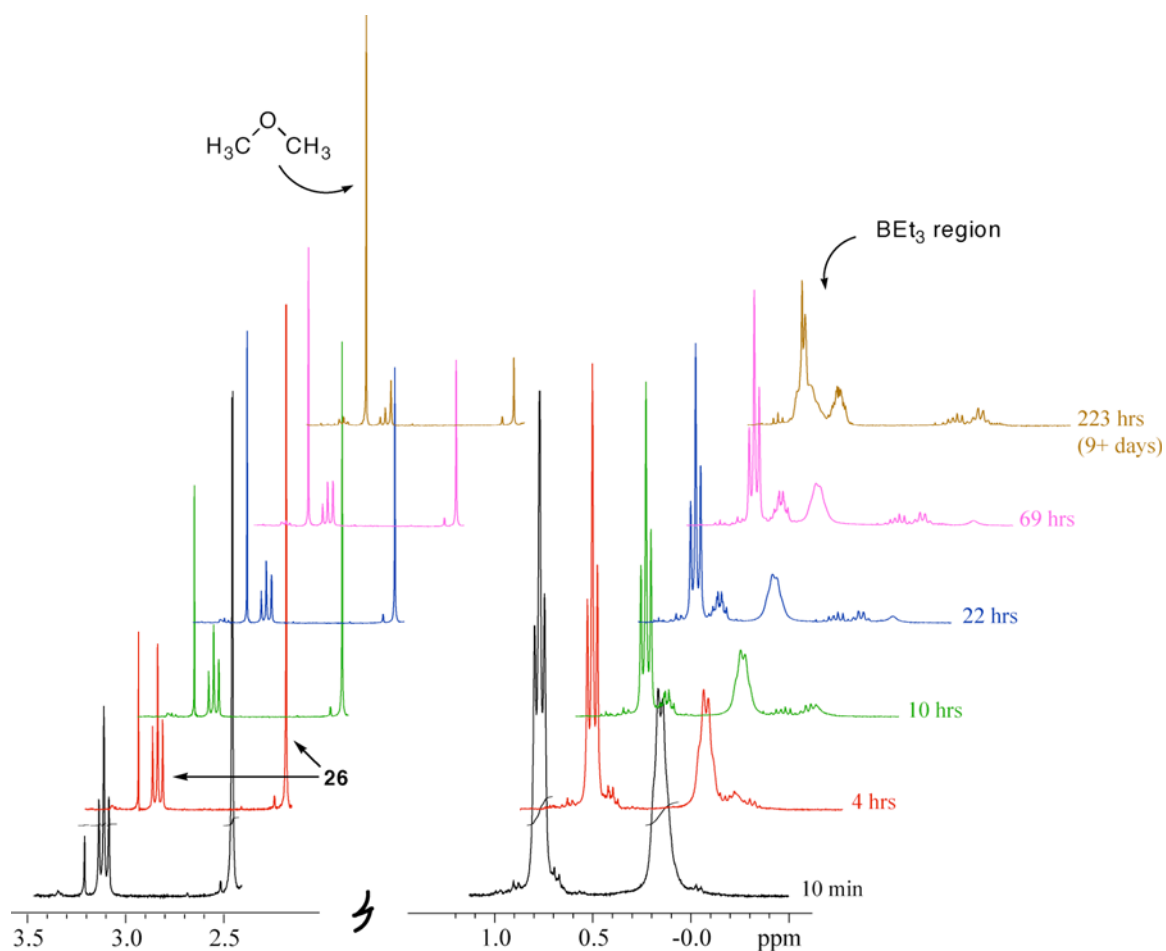
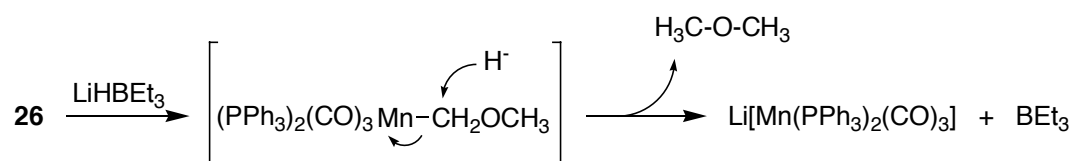


Figure 11. ^1H NMR spectra depicting generation of $(\text{CH}_3)_2\text{O}$ from **26** and NaBEt_3 over time.



Scheme 10. Proposed pathway for the release of dimethyl ether from **26** upon reaction with LiHBEt_3 .

Inspired by the highly extensive literature on migratory insertion chemistry with manganese alkyl complexes,⁶⁴⁻⁷⁰ the reactivity of complex **26** was investigated under an atmosphere of CO as a potential route to C_2 products derived from synthesis gas, such as

ethylene glycol. When a C_6D_6 solution of **26** was placed under one atmosphere of CO at room temperature, a slow reaction occurred that cleanly generated three manganese-containing products as observed by ^1H NMR (Figure 12). From the coupling to phosphorous and after verification using an original sample, one minor product was identified as methoxymethyl species **28**. The major product, as well as the other minor product, do not show coupling to phosphorous suggesting that acyl products or perhaps phosphine-free products were formed. $\text{Mn}(\text{CO})_5(\text{CH}_2\text{OCH}_3)$ was ruled out after a pure sample was prepared and compared to the ^1H NMR spectrum of the reaction.⁶⁴ A peak corresponding to free PPh_3 was observed in the ^{31}P NMR spectrum, however it was not known whether further loss of phosphine occurred from the manganese monophosphine species **28**. Furthermore, when a solution containing **26** and two equivalents of free PPh_3 were placed under CO, a similar distribution of products was obtained and no change in the rate of reaction was observed. As has been observed in analogous migratory insertion reactions, the reaction rate is increased when the reaction is carried out in THF.⁷¹

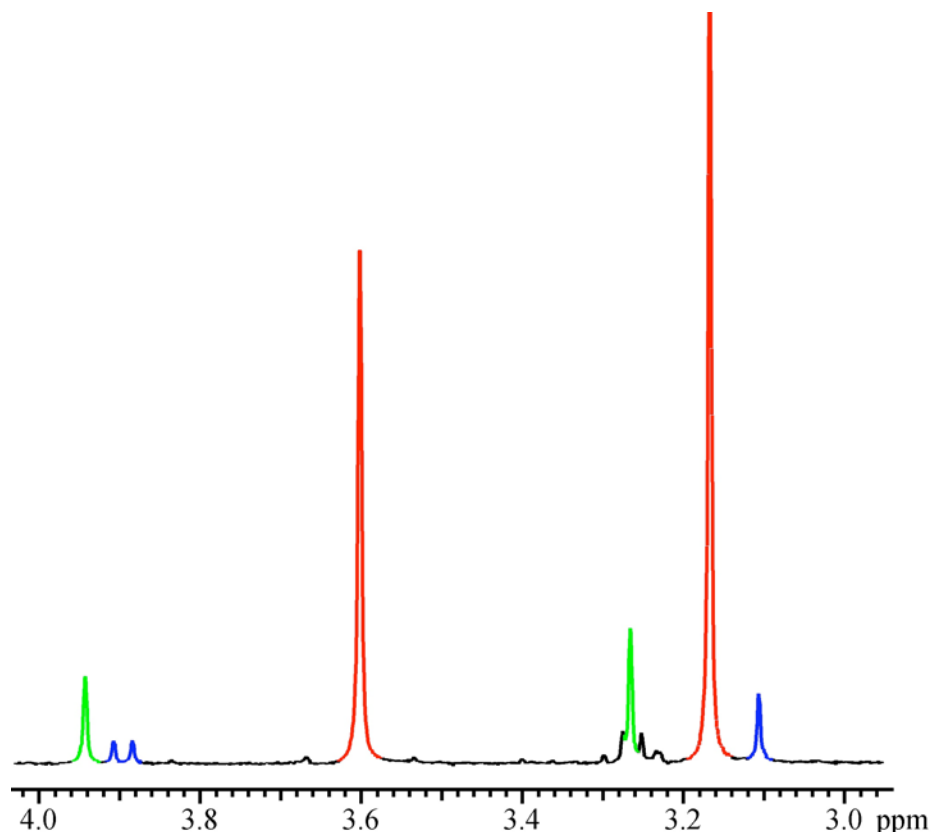
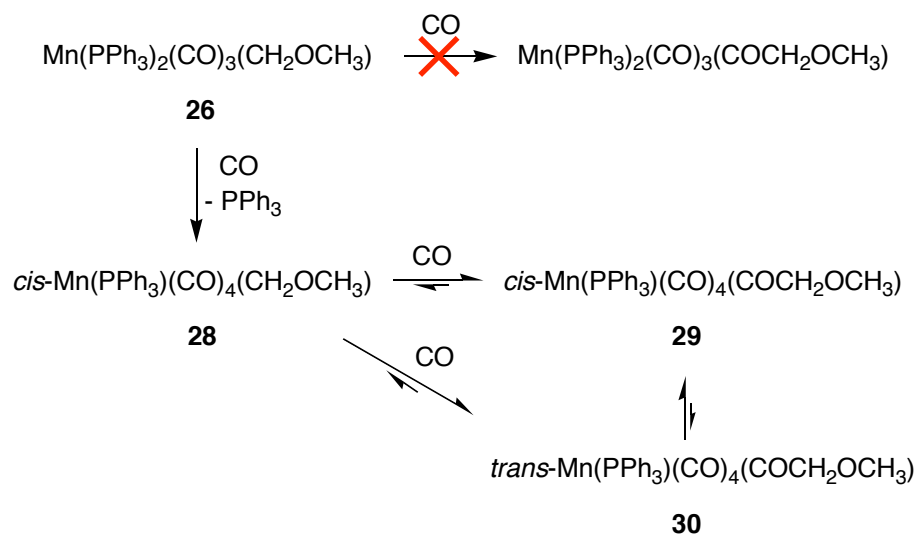


Figure 12. Methoxy and methylene region of the ^1H NMR spectrum of the product mixture of the reaction of **26** with 1 atm CO; **29** (red), **30** (green), and **28** (blue); traces of Et_2O in black.

As was mentioned previously, synthesizing **28** from the cationic carbonyl precursor **7** was not carried out here due to the rapid decomposition of the corresponding formyl intermediate from the first step to the manganese hydride complex. Despite this complication, complex **28** can be prepared *via* an alternate method involving the reaction of $\text{Na}[\text{Mn}(\text{PPh}_3)(\text{CO})_4]$ with $\text{ClCH}_2\text{OCH}_3$ in THF and obtained in excellent yield.⁷² This synthetic route was also employed in an alternate synthesis of **26**.

To obtain better insight on the identity of the reaction products, a similar carbonylation reaction was carried out using monophosphine **28**. After several days, identical product distribution and ratios were observed by ^1H NMR, however with no free PPh_3 . This result suggests that the carbonylation of **26** does not involve the formation of a

manganese bisphosphine acyl species but rather requires initial phosphine dissociation in the presence of CO. Moreover, **28** does not disproportionate in solution to give **26** and $\text{Mn(CO)}_5(\text{CH}_2\text{OCH}_3)$, further supporting this assertion. From the IR spectrum of the product mixture, the presence of $\text{Mn(CO)}_5(\text{COCH}_2\text{OCH}_3)$ can be ruled out, as the high frequency stretch expected for the complex (2130 cm^{-1}) is absent.⁶⁴ Definite identification of the two acyl products, as isomers *cis*- $\text{Mn(CO)}_4(\text{PPh}_3)(\text{COCH}_2\text{OCH}_3)$ (**29**) and *trans*- $\text{Mn(CO)}_4(\text{PPh}_3)(\text{COCH}_2\text{OCH}_3)$ (**30**) in a ratio of 100:16, was possible by the independent synthesis of the manganese monophosphine acyl complex from the reaction of $\text{Na[Mn(CO)}_4(\text{PPh}_3)]$ with $\text{ClC(O)CH}_2\text{OCH}_3$. In solution, the independently prepared acyl species also gave a mixture of the three products **29**, **30**, and **28** demonstrating the presence of equilibria between **28** and the acyl complexes (carbonylation/decarbonylation), as well as between **29** and **30**, as has been previously reported in the literature (Scheme 11).^{71,73} Furthermore, a ^{13}C NMR spectrum of the carbonylation reaction of **28** cleanly shows the growth of two diagnostic acyl peaks corresponding to **29** (272.8 ppm) and **30** (263.4 ppm) (Table 1).⁷⁴ Several attempts at growing crystals of **29** and **30** suitable for X-ray analysis were unsuccessful. Additionally, a preliminary attempt at methylating a mixture of **29** and **30** with methyl triflate to generate the corresponding carbene product was found inconclusive.



Scheme 11. Proposed mechanism for the carbonylation reaction of **26** and **28**.

Table 1. NMR^a and IR data for complexes **26**, **28**, **29** and **30**.

Complex	¹ H NMR (-OCH ₃ ; -CH ₂ -)	¹³ C NMR (-C(O)CH ₂ OCH ₃)	³¹ P NMR	IR ^b
26	2.73 (3H, s); 3.60 (2H, t, <i>J</i> _{HP} = 7.5 Hz)	-	76.6 (s)	2009, 1921, 1885
28	3.11 (3H, s); 3.90 (2H, d, <i>J</i> _{HP} = 7.0 Hz)	-	61.9 (s)	2062, 1982, 1967, 1936
29	3.17 (3H, s); 3.60 (2H, s)	272.78 (d, <i>J</i> _{CP} = 16.2 Hz)	53.5 (s)	2070, 1994, 1962, 1920, 1624
30	3.27 (3H, s); 3.94 (2H, s)	263.38 (s, br)	- ^c	-, ^d 1636

^a NMR data in ppm (C₆D₆). ^b CH₂Cl₂ solutions (cm⁻¹). ^c Signal was too small and broad to be observed. ^d Stretch from terminal CO not observed due to overlapping **29** stretches.

Conclusions and Outlook

A wide variety of Group 7 carbonyl derivatives have been studied to provide the tools necessary for the development of a system capable of catalyzing the transformation of synthesis gas to ethylene glycol. The manganese and rhenium complexes prepared are all six-coordinate species supported by carbonyl and phosphine ligands. Formyl complexes have been synthesized primarily using main group hydrides such as LiHBEt_3 , while the very electron-deficient **7** can be reduced using transition metal hydrides. Additionally, it was shown that by carrying out simple ligand modification, a diformyl species could be generated using complex **9**. Stable neutral carbenes have been synthesized by reacting the formyls with various boranes. Unfortunately, these novel compounds displayed limited reactivity.

Methylating rhenium and manganese formyls leads to the formation of stable methoxy carbenes. While limited reactivity was achieved that could lead to C-C coupled products directly, these complexes are easily reduced to the more reactive methoxymethyl species. Treating the manganese methoxymethyl complexes with a hydride source leads to the release of dimethyl ether in an $\text{S}_{\text{N}}2$ -type reaction involving hydride attack on the electrophilic methylene carbon. C-C bond formation was achieved under remarkably mild conditions by the carbonylation of the manganese methoxymethyl species leading to the formation of acyl complexes. Mechanistic insight was obtained by performing carbonylation reactions using various manganese methoxymethyl species. These studies determined that $\text{Mn}(\text{PPh}_3)_2(\text{CO})_3(\text{CH}_2\text{OCH}_3)$ does not undergo migratory insertion when exposed to CO, but rather requires initial ligand substitution to proceed. It

was also established that a dynamic equilibrium was present involving carbonylation/decarbonylation as well as the isomerization of the acyl product from a *cis* to a *trans* configuration.

Future work should certainly be aimed at further investigating mechanistic considerations of the migratory insertion reaction using the complexes presented herein, as well as performing kinetic studies that can lead to a better understanding of these systems.

Studies by Cutler and coworkers have demonstrated that migratory insertion involving methoxymethyl species of iron and cobalt was also possible, however both systems have limited catalytic utility.^{75,76} $\text{Ind}(\text{CO})_2\text{Fe}(\text{CH}_2\text{OCH}_3)$ (Ind = indenyl) requires initial formation of a bimetallic complex followed by treatment with CH_3I to induce carbonylation under CO.⁷⁶ On the other hand, $(\text{PMePh}_2)(\text{CO})_3\text{Co}(\text{CH}_2\text{OCH}_3)$ has not been shown to arise from simple transformations using the corresponding carbonyl precursor $\text{Co}(\text{PMePh}_2)(\text{CO})_4^+$.⁷⁵ In contrast, the manganese systems presented in this work show great promise as possible catalysts for the conversion of synthesis gas to ethylene glycol derivatives under remarkably mild conditions (1 atm CO, room temperature). Indeed, starting from the manganese carbonyl precursor, a possible catalytic cycle involving successive reduction/protonation and CO insertion steps can be envisioned (Schemes 5 and 6c). Obtaining the organic C_2 fragment from the acyl species requires straightforward steps reported previously.⁷⁶

Experimental Section

General Considerations. All air- and moisture-sensitive compounds were manipulated using standard vacuum line, Schlenk, or cannula techniques or in a glovebox under a nitrogen atmosphere. Solvents for air- and moisture-sensitive reactions were dried over sodium benzophenone ketyl, calcium hydride, or by the method of Grubbs. Benzene- d_6 was purchased from Cambridge Isotopes and dried over sodium benzophenone ketyl. Dichloromethane- d_2 was purchased from Cambridge Isotopes and distilled from calcium hydride. THF- d_8 was purchased from Cambridge Isotopes and dried either over sodium benzophenone ketyl or passed through a column of activated alumina. Other materials were used as received. $\text{Re}(\text{CO})_5\text{Br}$ and $\text{Mn}(\text{CO})_5\text{Br}$ were obtained from Strem, while $\text{ClCH}_2\text{OCH}_3$ and $\text{ClC}(\text{O})\text{CH}_2\text{OCH}_3$ were purchased from Aldrich. Preparations of $\text{Re}(\text{CO})_3(\text{PPh}_3)_2\text{Br}$,⁷⁷ **5**,³⁵ $\text{Mn}(\text{CO})_4(\text{PPh}_3)\text{Br}$,⁷⁸ **7**,³⁵ $\text{Mn}(\text{CO})_3(\text{PPh}_3)_2\text{Br}$,⁷⁷ **8**,³⁵ $[\text{Pt}(\text{dmpe})_2][\text{PF}_6]_2$,²⁹ $[\text{Pt}(\text{dmpe})_2(\text{H})][\text{PF}_6]$,²⁹ **24**,³⁶ **25**,³⁶ and **28**⁷² were carried out following modified procedures of previously reported syntheses.

Instrumentation. ^1H and ^{31}P NMR spectra were recorded on a Varian Mercury 300 spectrometer at 299.868 MHz and 121.389 MHz respectively, at room temperature. ^{13}C NMR spectra were recorded on a Varian INOVA-500 spectrometer at 125.903 MHz at room temperature. All ^1H NMR chemical shifts are reported relative to TMS, and ^1H (residual) chemical shifts of the solvent are used as secondary standard. ^{13}C NMR chemical shifts are reported relative to the internal solvent. ^{31}P NMR chemical shifts are reported relative to an external H_3PO_4 (85%) standard. ^{19}F NMR chemical shifts are reported relative to an external CCl_3F standard. Elemental analyses were performed by

Desert Analytics, Tuscon, AZ. X-ray crystallography was carried out by Dr. Michael W. Day and Lawrence M. Henling using an Enraf-Nonius CAD-4 diffractometer. IR spectra were recorded on a Nicolet 6700 FT-IR spectrometer. High-pressure NMR experiments were carried out using similar equipment and procedures as described previously.⁷⁹

Synthesis of $\text{Re}(\text{CO})_3(\text{PPh}_3)_2\text{Br}$. To a 80 mL flask was added $\text{Re}(\text{CO})_5\text{Br}$ (0.663 g, 1.632 mmol), PPh_3 (0.942 g, 3.591 mmol) and toluene (30 mL). The flask was sealed and placed in a 110°C oil bath with heavy stirring for 15 hrs. After reaction completion, the insoluble product is decanted and recrystallized from CH_2Cl_2 / petroleum ether to give 1.223 g of the desired product as a white solid in 86 % yield. ^1H NMR (RT, 300 MHz, CD_2Cl_2): δ = 7.38 – 7.46 (18H, m, *ArH*), 7.62 – 7.72 (12H, m, *ArH*). ^{31}P NMR (RT, 121 MHz, CD_2Cl_2): δ = 6.8 ppm (s). HRMS (FAB+) m/z calcd for $\text{C}_{38}\text{H}_{30}\text{BrO}_2\text{P}_2\text{Re}$ (M-CO) 846.0462, found 846.0466.

Synthesis of $[\text{Re}(\text{CO})_4(\text{PPh}_3)_2][\text{BF}_4]$ (5**).** To a 80 mL flask was added $\text{Re}(\text{CO})_3(\text{PPh}_3)_2\text{Br}$ (0.186 g, 0.2126 mmol), AgBF_4 (0.054 g, 0.2774 mmol) and CH_2Cl_2 (20 mL). On the Schlenk line, the flask was first degassed and then placed under an atmosphere of CO and sealed. The reaction was allowed to stir for 15 hrs. After reaction completion, the mixture was filtered through a Celite pad. The filtrate was placed under vacuum to reduce the volume and layered with petroleum ether, which precipitated 0.178 g of **5** as a white solid in 95 % yield. ^1H NMR (RT, 300 MHz, CD_2Cl_2): δ = 7.44 – 7.61 (30H, m, *ArH*). ^{31}P NMR (RT, 121 MHz, CD_2Cl_2): δ = 4.3 ppm (s). IR: ν_{CO} (cm^{-1} , CH_2Cl_2) 2000. HRMS (FAB+) m/z calcd for $\text{C}_{40}\text{H}_{30}\text{ReP}_2\text{O}_4$ 823.1177, found 823.1183.

Synthesis of $\text{Re}(\text{CO})_3(\text{dppe})\text{Br}$. To a 80 mL flask was added $\text{Re}(\text{CO})_5\text{Br}$ (0.742 g, 1.827 mmol), dppe (0.800 g, 2.008 mmol) and toluene (30 mL). The flask was sealed and placed in a 110°C oil bath with heavy stirring for 15 hrs. After reaction completion, the mixture was filtered and the filtrate dried under vacuum. The resulting residue was recrystallized from CH_2Cl_2 /Petroleum ether to give 0.988 g of the desired product as a white solid in 72 % yield. ^1H NMR (RT, 300 MHz, CD_2Cl_2): δ = 2.58 – 2.82 (2H, m, CH_2), 2.95 – 3.19 (2H, m, CH_2), 7.37 – 7.50 (12H, m, ArH), 7.52 – 7.69 (8H, m, ArH). ^{31}P NMR (RT, 121 MHz, CD_2Cl_2): δ = 28.7 ppm (s). HRMS (FAB+) m/z calcd for $\text{C}_{29}\text{H}_{24}\text{BrO}_3\text{P}_2\text{Re}$ 747.9942, found 747.9910.

Synthesis of $[\text{Re}(\text{CO})_4(\text{dppe})][\text{BF}_4]$ (6**).** To a 80 mL flask was added $\text{Re}(\text{CO})_3(\text{dppe})\text{Br}$ (0.198 g, 0.2645 mmol), AgBF_4 (0.067 g, 0.3442 mmol) and CH_2Cl_2 (20 mL). On the Schlenk line, the flask was first degassed and then placed under an atmosphere of CO and sealed. The reaction was allowed to stir for 15 hrs. After reaction completion, the mixture was filtered through a Celite pad. The filtrate was placed under vacuum to reduce the volume and layered with petroleum ether, which precipitated 0.162 g of **6** as a white solid in 81 % yield. ^1H NMR (RT, 300 MHz, CD_2Cl_2): δ = 3.24 – 3.45 (4H, m, CH_2), 7.45 – 7.67 (20H, m, ArH). IR: ν_{CO} (cm^{-1} , CH_2Cl_2) 2112, 2033, 2017, 2007. HRMS (FAB+) m/z calcd for $\text{C}_{30}\text{H}_{24}\text{O}_4\text{P}_2\text{Re}$ 697.0708, found 697.0708.

Synthesis of $\text{Mn}(\text{CO})_5\text{Br}$. In a flask, $\text{Mn}_2(\text{CO})_{10}$ (2.510 g, 6.436 mmol) was dissolved in CH_2Cl_2 (30 mL) and placed on the Schlenk line under argon. Br_2 (0.45 mL, 8.783 mmol, 1.4 equiv.) was syringed into the flask. The mixture color went from yellow to orange-red. The reaction was stirred for 3 hrs, after which the solvent and excess Br_2 were

removed in vacuo. The resulting solid was washed with petroleum ether in the glovebox and dried under vacuum to give 3.463 g of the orange product in 98 % yield. IR: ν_{CO} (cm^{-1} , CH_2Cl_2) 2138, 2048, 2007.

Synthesis of $\text{Mn}(\text{CO})_4(\text{PPh}_3)\text{Br}$. $\text{Mn}(\text{CO})_5\text{Br}$ (1.024 g, 3.725 mmol) and PPh_3 (0.977 g, 3.725 mmol) were placed in a flask and dissolved in CH_2Cl_2 (20 mL) to give an orange mixture. The flask was sealed, degassed and placed in an oil bath heated to 42°C . After 3 hrs, the solvent was removed in vacuo to give an orange residue. In the glovebox, the mixture was recrystallized from CH_2Cl_2 / petroleum ether to give 1.707 g of the product as a yellow solid in 90 % yield. ^1H NMR (RT, 300 MHz, CH_2Cl_2): $\delta = 7.40 - 7.54$ (9H, m, Ar-*H*), $7.63 - 7.72$ (6H, m, Ar-*H*). ^{31}P NMR (RT, 121 MHz, CH_2Cl_2): $\delta = 41.3$ ppm (s, br). IR: ν_{CO} (cm^{-1} , CH_2Cl_2) 2090, 2017, 2006, 1961. HRMS (FAB+) m/z calcd for $\text{C}_{22}\text{H}_{15}\text{BrMnO}_4\text{P}$ 507.9272, found 507.9279.

Synthesis of $[\text{Mn}(\text{CO})_5(\text{PPh}_3)][\text{BF}_4]$ (7**).** To a 80 mL flask was added $\text{Mn}(\text{CO})_4(\text{PPh}_3)\text{Br}$ (1.266 g, 2.486 mmol), AgBF_4 (0.629 g, 3.231 mmol, 1.3 equiv.) and CH_2Cl_2 (20 mL). On the Schlenk line, the flask was first degassed and then placed under an atmosphere of CO and sealed. The reaction was allowed to stir for 15 hrs. After reaction completion, the mixture was filtered through a Celite pad. The yellow filtrate was placed under vacuum to reduce the volume and layered with petroleum ether, which precipitated 1.150 g of **7** as a yellow solid in 85 % yield. ^1H NMR (RT, 300 MHz, CD_2Cl_2): $\delta = 7.42 - 7.73$ (15H, m, Ar-*H*). ^{31}P NMR (RT, 121 MHz, CD_2Cl_2): $\delta = 42.7$ ppm (s, v br). IR: ν_{CO} (cm^{-1} , CH_2Cl_2) 2142, 2065, 2051. HRMS (FAB+) m/z calcd for $\text{C}_{23}\text{H}_{15}\text{MnO}_5\text{P}$ 457.0038, found 457.0019.

Synthesis of $\text{Mn}(\text{CO})_3(\text{PPh}_3)_2\text{Br}$. $\text{Mn}(\text{CO})_5\text{Br}$ (0.524 g, 1.906 mmol) and PPh_3 (1.212 g, 4.621 mmol) were placed in a flask and dissolved in CH_2Cl_2 (20 mL) to give an orange mixture. The flask was sealed, degassed and placed in an oil bath heated to 42°C . After 10 days, the flask contained a yellow precipitate in an orange solution. In the glovebox, the precipitate was filtered and washed with petroleum ether. The volume of the filtrate was reduced and petroleum ether was added to crash out a second batch of yellow solid. Yield: 0.701 g (50 %). ^1H NMR (RT, 300 MHz, CH_2Cl_2): $\delta = 7.37 - 7.44$ (18H, m, Ar-*H*), $7.70 - 7.78$ (12H, m, Ar-*H*). ^{31}P NMR (RT, 121 MHz, CH_2Cl_2): $\delta = 54.8$ ppm (s, br). IR: ν_{CO} (cm^{-1} , CH_2Cl_2) 2037, 1950, 1917. HRMS (FAB+) m/z calcd for $\text{C}_{36}\text{H}_{30}\text{MnP}_2^{81}\text{Br}$ ($\text{M}-(\text{CO})_3$) 660.0366, found 660.0372.

Synthesis of $[\text{Mn}(\text{CO})_4(\text{PPh}_3)_2][\text{BF}_4]$ (8**).** To a 80 mL flask was added $\text{Mn}(\text{CO})_3(\text{PPh}_3)_2\text{Br}$ (0.687 g, 0.9241 mmol), AgBF_4 (0.234 g, 1.202 mmol, 1.3 equiv.) and CH_2Cl_2 (20 mL). On the Schlenk line, the flask was first degassed and then placed under an atmosphere of CO and sealed. The reaction was allowed to stir for 15 hrs. After reaction completion, the mixture was filtered through a Celite pad and washed with CH_2Cl_2 . The yellow filtrate was placed under vacuum to reduce the volume and layered with petroleum ether, which precipitated 0.551 g of **8** as a pale yellow solid in 77 % yield. ^1H NMR (RT, 300 MHz, CD_2Cl_2): $\delta = 7.48 - 7.65$ (30H, m, Ar*H*). ^{31}P NMR (RT, 121 MHz, CD_2Cl_2): $\delta = 53.3$ ppm (s, br). IR: ν_{CO} (cm^{-1} , CH_2Cl_2) 2001. HRMS (FAB+) m/z calcd for $\text{C}_{40}\text{H}_{30}\text{MnO}_4\text{P}_2$ 691.1000, found 691.1021.

Synthesis of $\text{Re}(\text{CO})_3(\text{P}(\text{C}_6\text{H}_4(p\text{-CF}_3))_3)_2\text{Br}$. To a 80 mL flask was added $\text{Re}(\text{CO})_5\text{Br}$ (0.655 g, 1.613 mmol), $\text{P}(\text{C}_6\text{H}_4(p\text{-CF}_3))_3$ (1.504 g, 3.226 mmol) and toluene (30 mL). The flask was sealed and placed in a 110°C oil bath with heavy stirring. After 4 days, the flask was degassed and placed back into the oil bath. After stirring for 7 more days, the solvent was removed in vacuo and the resulting mixture washed several times with CH_2Cl_2 to give 1.690 g of the desired product as a white solid in 82 % yield. ^1H NMR (RT, 300 MHz, CD_2Cl_2): $\delta = 7.71 - 7.86$ (24H, m, ArH). ^{31}P NMR (RT, 121 MHz, CD_2Cl_2): $\delta = 7.2$ ppm (s). ^{19}F NMR (RT, 471 MHz, CD_2Cl_2): $\delta = -63.9$ ppm (18F, s, CF_3). IR: ν_{CO} (cm^{-1} , CH_2Cl_2) 2063, 1963, 1920. HRMS (FAB+) m/z calcd for $\text{C}_{45}\text{H}_{24}\text{BrP}_2\text{O}_3\text{F}_{18}\text{Re}$ 1281.966, found 1281.967.

Synthesis of $[\text{Re}(\text{CO})_4(\text{P}(\text{C}_6\text{H}_4(p\text{-CF}_3))_3)_2][\text{BF}_4]$ (9**).** To a 80 mL flask was added $\text{Re}(\text{CO})_3(\text{P}(\text{C}_6\text{H}_4(p\text{-CF}_3))_3)_2\text{Br}$ (1.076 g, 0.8389 mmol), AgBF_4 (0.212 g, 1.089 mmol, 1.3 equiv.) and CH_2Cl_2 (30 mL). On the Schlenk line, the flask was first degassed and then placed under an atmosphere of CO and sealed. The reaction was allowed to stir for 15 hrs. After reaction completion, the solvent was removed in vacuo and the product dissolved in CH_3CN . The mixture was then filtered through a Celite pad under air. The filtrate was placed under vacuum to reduce the volume and layered with petroleum ether, which precipitated 0.944 g of **9** as a white solid in 85 % yield. The crystalline product was dried on the high vacuum line overnight. ^1H NMR (RT, 300 MHz, CD_3CN): $\delta = 7.73 - 7.82$ (12H, m, ArH), $7.86 - 7.95$ (12H, m, ArH). ^{31}P NMR (RT, 121 MHz, CD_3CN): $\delta = 7.4$ ppm (s). ^{19}F NMR (RT, 471 MHz, CD_3CN): $\delta = -63.2$ (18F, s, CF_3), -151.2 (4F, s, BF_4^-). IR: ν_{CO} (cm^{-1} , CH_3CN) 2017. HRMS (FAB+) m/z calcd for $\text{C}_{46}\text{H}_{24}\text{ReP}_2\text{O}_4\text{F}_{18}$ 1231.042, found 1231.041.

NMR scale preparation of $\text{Re}(\text{CO})_3(\text{PPh}_3)_2(\text{CHO})$ (10). $[\text{Re}(\text{CO})_4(\text{PPh}_3)_2][\text{BF}_4]$ (0.019 g, 0.02155 mmol) was placed in a J-Young NMR tube and suspended in $\text{THF-}d_8$ (0.7 mL). LiHBEt_3 (1 M in THF, 22 μL , 1 equiv.) was syringed into the tube. The sealed tube was shaken vigorously to give a yellow solution. ^1H NMR (RT, 300 MHz, $\text{THF-}d_8$): δ = 7.32 – 7.43 (18H, m, *ArH*), 7.45 – 7.56 (12H, m, *ArH*), 13.86 (1H, s, *CHO*). ^{31}P NMR (RT, 121 MHz, $\text{THF-}d_8$): δ = 13.2 ppm (s).

NMR scale preparation of *fac*- $\text{Re}(\text{CO})_3(\text{dppe})(\text{CHO})$. $[\text{Re}(\text{CO})_4(\text{dppe})][\text{BF}_4]$ (0.012 g, 0.01549 mmol) was placed in a J-Young NMR tube and suspended in $\text{THF-}d_8$ (0.7 mL). LiHBEt_3 (1 M in THF, 16 μL , 1 equiv.) was syringed into the tube. The sealed tube was shaken vigorously to give a yellow solution of the desired formyl species. ^1H NMR (RT, 300 MHz, $\text{THF-}d_8$): δ = 2.81 – 3.22 (4H, m, CH_2), 7.31 – 7.46 (12H, m, *ArH*), 7.49 – 7.66 (8H, m, *ArH*), 12.89 (1H, t, J_{HP} = 3.7 Hz, *CHO*), 14.71 (dd, J_{HP} = 10.9 Hz, $J_{\text{HP}} < 1$ Hz, minor *mer* product). ^{31}P NMR (RT, 121 MHz, $\text{THF-}d_8$): δ = 36.7 ppm (s).

NMR scale preparation of $\text{Cr}(\text{CO})_5(\text{CHO})$. $\text{Cr}(\text{CO})_6$ (0.016 g, 0.07271 mmol) was placed in a J-Young NMR tube and suspended in $\text{THF-}d_8$ (0.7 mL). LiHBEt_3 (1 M in THF, 73 μL , 1 equiv.) was syringed into the tube. The sealed tube was shaken vigorously to give a yellow-orange solution. ^1H NMR (RT, 300 MHz, $\text{THF-}d_8$): δ = 14.77 (1H, s, *CHO*).

Synthesis of $\text{Cr}(\text{CO})_4(\text{dppe})$. To a 80 mL flask was added $\text{Cr}(\text{CO})_6$ (0.732 g, 3.326 mmol) and dissolved in toluene (20 mL). The flask was placed in a 110°C oil bath. The

reaction was allowed to stir for 36 hrs. After reaction completion, the solvent was evacuated and the residue recrystallized from CH₂Cl₂ / petroleum ether to give 1.528 g of the desired product as yellowish crystals in 82 % yield. ¹H NMR (RT, 300 MHz, CDCl₃): δ = 2.47 – 2.70 (4H, m, CH₂), 7.30 – 7.43 (12H, m, ArH), 7.48 – 7.62 (8H, m, ArH). ³¹P NMR (RT, 121 MHz, CDCl₃): δ = 80.1 ppm (s). IR: ν_{CO} (cm⁻¹, CH₂Cl₂) 2009, 1910, 1900, 1878. HRMS (FAB+) *m/z* calcd for C₃₀H₂₄CrO₄P₂ 562.0555, found 562.0565.

NMR scale reduction of [Mn(CO)₅(PPh₃)] [BF₄] at room temperature.

[Mn(CO)₅(PPh₃)] [BF₄] (0.012 g, 0.02114 mmol) was placed in a J-Young NMR tube and suspended in THF-*d*₈ (0.7 mL). LiHBEt₃ (1 M in THF, 21 μL, 1 equiv.) was syringed into the tube. The sealed tube was shaken vigorously to give a yellow solution, which contained Mn(CO)₄(PPh₃)(CHO) and Mn(CO)₄(PPh₃)(H) in a 3:7 ratio, respectively. ¹H NMR (RT, 300 MHz, THF-*d*₈): δ = -7.26 (d, *J*_{HP} = 33.6 Hz, Mn-*H*), 7.23 – 7.74 (m, ArH), 13.59 (d, *J*_{HP} = 2.3 Hz, CHO). ³¹P NMR (RT, 121 MHz, THF-*d*₈): δ = -4.5 (s, free PPh₃), 57.2 (s, br), 66.5 (s, br).

NMR scale reduction of [Mn(CO)₅(PPh₃)] [BF₄] at low temperature.

[Mn(CO)₅(PPh₃)] [BF₄] (0.011 g, 0.01930 mmol) was placed in a J-Young NMR tube and suspended in THF-*d*₈ (0.4 mL). The suspension was frozen in the cold well. Fresh THF-*d*₈ was added to the top of the layer and frozen. Finally, LiHBEt₃ (1 M in THF, 20 μL, 1 equiv.) was syringed into the tube and frozen as well. Outside the glovebox, the tube was placed in a -78°C bath until ready to collect data. The tube was thawed and shaken vigorously right before placing it into the NMR probe giving a yellow solution, which contained *cis*-Mn(CO)₄(PPh₃)(CHO), *trans*-Mn(CO)₄(PPh₃)(CHO) and

Mn(CO)₄(PPh₃)(H) in a 10.5:1:3 ratio, respectively. ¹H NMR (RT, 300 MHz, THF-*d*₈): δ = -7.26 (d, *J*_{HP} = 33.6 Hz, Mn-*H*), 7.23 – 7.74 (m, *ArH*), 13.59 (d, *J*_{HP} = 2.3 Hz, *cis*-CHO), 14.37 (d, *J*_{HP} = 9.0 Hz, *trans*-CHO). ³¹P NMR (RT, 121 MHz, THF-*d*₈): δ = 57.2 (s, br).

NMR scale reduction of [Mn(CO)₅(PPh₃)] [BF₄] under CO. [Mn(CO)₅(PPh₃)] [BF₄] (0.012 g, 0.02206 mmol) was placed in a J-Young NMR tube and suspended in THF-*d*₈ (0.4 mL). The suspension was frozen in the cold well. Fresh THF-*d*₈ was added to the top of the layer and frozen. Finally, LiHBET₃ (1 M in THF, 22 μL, 1 equiv.) was syringed into the tube and frozen as well. On the Schlenk line, the tube was placed under 1 atmosphere of CO and warmed to room temperature. The yellow solution contained *cis*-Mn(CO)₄(PPh₃)(CHO), *trans*-Mn(CO)₄(PPh₃)(CHO) and Mn(CO)₄(PPh₃)(H) in a 14:1:7 ratio, respectively. ¹H NMR (RT, 300 MHz, THF-*d*₈): δ = -7.26 (d, *J*_{HP} = 33.6 Hz, Mn-*H*), 7.23 – 7.74 (m, *ArH*), 13.59 (d, *J*_{HP} = 2.3 Hz, *cis*-CHO), 14.37 (d, *J*_{HP} = 9.0 Hz, *trans*-CHO). ³¹P NMR (RT, 121 MHz, THF-*d*₈): δ = 57.2 (s, br).

NMR scale reduction of [Mn(CO)₅(PPh₃)] [BF₄] using [Pt(dmpe)₂(H)] [PF₆] at room temperature. [Mn(CO)₅(PPh₃)] [BF₄] (0.013 g, 0.02389 mmol) and [Pt(dmpe)₂(H)] [PF₆] (0.015 g, 0.02389 mmol) were placed in a J-Young NMR tube and suspended in THF-*d*₈ (0.7 mL). The tube was sealed and shaken vigorously to give a yellow solution containing *cis*-Mn(CO)₄(PPh₃)(CHO), *trans*-Mn(CO)₄(PPh₃)(CHO) and Mn(CO)₄(PPh₃)(H) in a 11:1.5:1 ratio, respectively, as well as other unidentified decomposition products. ¹H NMR (RT, 300 MHz, THF-*d*₈): δ = -7.26 (d, *J*_{HP} = 33.6 Hz, Mn-*H*), 7.32 – 7.74 (m,

ArH), 13.59 (d, $J_{\text{HP}} = 2.3$ Hz, *cis*-CHO), 14.37 (d, $J_{\text{HP}} = 9.0$ Hz, *trans*-CHO). ^{31}P NMR (RT, 121 MHz, THF- d_8): $\delta = 57.2$ (s, br).

After 2.5 hrs, the ^1H NMR spectrum shows that the products are now in 7:1:3.5 ratio, demonstrating that the formyl decomposes to the hydride via loss of CO.

NMR scale preparation of $\text{Mn}(\text{CO})_3(\text{PPh}_3)_2(\text{CHO})$ (11). $[\text{Mn}(\text{CO})_4(\text{PPh}_3)_2][\text{BF}_4]$ (0.005 g, 0.00642 mmol) was placed in a J-Young NMR tube and suspended in THF- d_8 (0.7 mL). LiHBEt_3 (1 M in THF, 6 μL , 1 equiv.) was syringed into the tube. The sealed tube was shaken vigorously to give a yellow solution. ^1H NMR (RT, 300 MHz, THF- d_8): $\delta = 7.17 - 7.68$ (30H, m, ArH), 13.55 (1H, t, $J_{\text{HP}} = 2.0$ Hz, CHO).

NMR scale preparation of $\text{Re}(\text{CO})_3(\text{P}(\text{C}_6\text{H}_4(p\text{-CF}_3))_3)_2(\text{CHO})$ (14). $[\text{Re}(\text{CO})_4(\text{P}(\text{C}_6\text{H}_4(p\text{-CF}_3))_3)_2][\text{BF}_4]$ (0.014 g, 0.01063 mmol) was placed in a J-Young NMR tube and suspended in THF- d_8 (0.7 mL). LiHBEt_3 (1 M in THF, 11 μL , 1 equiv.) was syringed into the tube. The sealed tube was shaken vigorously to give a yellowish solution. ^1H NMR (RT, 300 MHz, THF- d_8): $\delta = 7.71 - 7.83$ (24H, m, ArH), 14.58 (1H, s, CHO). ^{31}P NMR (RT, 121 MHz, THF- d_8): $\delta = 16.8$ ppm (s).

NMR scale preparation of $\text{Li}[\text{Re}(\text{CO})_2(\text{P}(\text{C}_6\text{H}_4(p\text{-CF}_3))_3)_2(\text{CHO})_2]$ (15). $[\text{Re}(\text{CO})_4(\text{P}(\text{C}_6\text{H}_4(p\text{-CF}_3))_3)_2][\text{BF}_4]$ (0.005 g, 0.00379 mmol) was placed in a J-Young NMR tube and suspended in THF- d_8 (0.7 mL). LiHBEt_3 (1 M in THF, 15 μL , 0.0152 mmol, 4 equiv.) was syringed into the tube. The sealed tube was shaken vigorously to give a yellowish solution. ^1H NMR (RT, 300 MHz, THF- d_8): $\delta = 7.60 - 7.68$ (24H, m, ArH), 14.66 (2H, s, CHO). ^{31}P NMR (RT, 121 MHz, THF- d_8): $\delta = 24.7$ ppm (s).

Synthesis of $\text{Re}(\text{CO})_3(\text{dppe-F}_{20})\text{Br}$. To a 80 mL flask was added $\text{Re}(\text{CO})_5\text{Br}$ (0.384 g, 0.9454 mmol), dppe-F_{20} (0.717 g, 0.9454 mmol) and toluene (30 mL). The flask was sealed and placed in a 110°C oil bath with heavy stirring for 15 hrs. After reaction completion, the solvent was evacuated. The resulting residue was recrystallized from CH_2Cl_2 /Petroleum ether to give 0.773 g of the desired product as a white solid in 74 % yield. ^1H NMR (RT, 300 MHz, CD_2Cl_2): δ = 2.98 – 3.24 (2H, m, CH_2), 3.33 – 3.59 (2H, m, CH_2). ^{31}P NMR (RT, 121 MHz, CD_2Cl_2): δ = 6.2 ppm (s). ^{19}F NMR (RT, 471 MHz, CD_2Cl_2): δ = -128.6 (8F, m, ArF), -146.6 (4F, m, ArF), -159.6 (8F, m, ArF). HRMS (FAB+) m/z calcd for $\text{C}_{29}\text{H}_4\text{BrF}_{20}\text{P}_2\text{O}_3$ 1107.806, found 1107.806.

Synthesis of $[\text{Re}(\text{CO})_4(\text{dppe-F}_{20})][\text{BF}_4]$ (16**).** To a 80 mL flask was added $\text{Re}(\text{CO})_3(\text{dppe-F}_{20})\text{Br}$ (0.197 g, 0.1777 mmol), AgBF_4 (0.045 g, 0.2312 mmol) and CH_2Cl_2 (20 mL). On the Schlenk line, the flask was first degassed and then placed under an atmosphere of CO and sealed. The reaction was allowed to stir for 15 hrs. After reaction completion, the mixture was filtered through a Celite pad. The filtrate was placed under vacuum to reduce the volume and layered with petroleum ether, which precipitated 0.110 g of **16** as a white solid in 54 % yield. ^1H NMR (RT, 300 MHz, CD_2Cl_2): δ = 3.39 – 3.49 (2H, m, CH_2), 3.51 – 3.60 (2H, m, CH_2). ^{31}P NMR (RT, 121 MHz, CD_2Cl_2): δ = 1.8 ppm (s). ^{19}F NMR (RT, 471 MHz, CD_2Cl_2): δ = -129.7 (8F, m, ArF), -143.6 (4F, m, ArF), -153.6 (4F, BF_4^-), -157.6 (8F, m, ArF). HRMS (FAB+) m/z calcd for $\text{C}_{30}\text{H}_4\text{F}_{20}\text{P}_2\text{O}_4\text{Re}$ 1056.882, found 1056.884.

Synthesis of $\text{Re}(\text{CO})_3(\text{PPh}_3)_2(\text{CHOBf}_3)$ (17). *Method A:* In the glovebox, a suspension of $[\text{Re}(\text{CO})_4(\text{PPh}_3)_2][\text{BF}_4]$ (0.125 g, 0.1418 mmol) in THF (3 mL) was stirred in a vial. LiHBEt_3 (1 M in THF, 142 μL , 1 equiv.) was syringed in to give a yellow solution after filtration. THF was evacuated to give the crude formyl species and LiBF_4 byproduct as a yellow residue. TMSOTf (21 μL , ca. 1 equiv.) was dissolved in CH_2Cl_2 (5 mL) and added to the residue and stirred for 5 minutes, after which the solvent was evacuated. Colorless crystals of the product were obtained upon recrystallization with CH_2Cl_2 / petroleum ether. Yield: 0.072 g (60 %). ^1H NMR (RT, 300 MHz, CD_2Cl_2): δ = 7.32 – 7.64 (30H, m, *ArH*), 13.38 (1H, s, *CHOBf*₃). ^{13}C NMR (RT, 126 MHz, CD_2Cl_2): δ = 129.3 (t, J_{CP} = 5.1 Hz, *Ar*), 131.3 (s, *Ar*), 133.4 (t, J_{CP} = 5.7 Hz, *Ar*), 134.8 (t, J_{CP} = 25.5 Hz, *Ar*), 192.9 (t, J_{CP} = 8.3 Hz, *cis* CO's), 196.1 (t, J_{CP} = 8.1 Hz, *trans* CO), 300.7 (s, *CHOBf*₃). ^{31}P NMR (RT, 121 MHz, CD_2Cl_2): δ = 12.6 ppm (s). ^{19}F NMR (RT, 471 MHz, CD_2Cl_2): δ = -156.5 ppm (s). IR: ν_{CO} (cm^{-1} , CH_2Cl_2) 2063, 2003, 1964. HRMS (FAB+) m/z calcd for $\text{C}_{40}\text{H}_{31}\text{BF}_2\text{O}_4\text{P}_2\text{Re}$ (M-F) 873.1317, found 873.1331; for $\text{C}_{40}\text{H}_{30}\text{O}_4\text{P}_2\text{Re}$ (M-BF₃-H) 823.1177, found 823.1055.

Method B: In the glovebox, a suspension of $[\text{Re}(\text{CO})_4(\text{PPh}_3)_2][\text{BF}_4]$ (0.333 g, 0.3777 mmol) in THF (3 mL) was stirred in a vial. LiHBEt_3 (1 M in THF, 378 μL , 1 equiv.) was syringed in to give a yellow solution after filtration. THF was evacuated to give the crude formyl species and LiBF_4 byproduct as a yellow residue. $\text{BF}_3\cdot\text{OEt}_2$ (62 μL , 1.3 equiv.) was dissolved in CH_2Cl_2 (5 mL) and added to the residue and stirred for 5 minutes, after which the solvent was evacuated. The solid was recrystallized from CH_2Cl_2 / petroleum ether to give 0.292 g of a white crystalline solid in 90 % yield.

Synthesis of $\text{Re}(\text{CO})_3(\text{PPh}_3)_2(\text{CHOB}(\text{C}_6\text{F}_5)_3)$ (18). In the glovebox, a suspension of $[\text{Re}(\text{CO})_4(\text{PPh}_3)_2][\text{BF}_4]$ (0.187 g, 0.2121 mmol) in THF (3 mL) was stirred in a vial. LiHBEt_3 (1 M in THF, 212 μL , 1 equiv.) was syringed in to give a yellow solution after filtration. THF was evacuated to give the crude formyl species and LiBF_4 byproduct as a yellow residue. $\text{B}(\text{C}_6\text{F}_5)_3$ (0.109 g, 0.2129 mmol) was dissolved in CH_2Cl_2 (5 mL) and added to the residue and stirred for 5 minutes, after which the solvent was evacuated. The solid was recrystallized from THF / petroleum ether to give 0.125 g of a white crystalline solid in 45 % yield. Anal. Calcd. for $\text{C}_{58}\text{H}_{31}\text{BF}_{15}\text{O}_4\text{P}_2\text{Re}$: C, 52.15; H, 2.34. Found: C, 52.85; H, 2.34. ^1H NMR (RT, 300 MHz, CD_2Cl_2): δ = 7.30 – 7.47 (30H, m, *ArH*), 13.84 (1H, s, *CHOB*(C_6F_5)₃). ^{13}C NMR (RT, 126 MHz, CD_2Cl_2): δ = 118.2 (m, $\text{B}(\text{C}_6\text{F}_5)$), 129.0 (t, J_{CP} = 5.0 Hz, *Ar*), 131.2 (s, *Ar*), 133.4 (t, J_{CP} = 5.5 Hz, *Ar*), 134.6 (t, J_{CP} = 24.4 Hz, *Ar*), 137.3 (dm, J_{CF} = 250 Hz, $\text{B}(\text{C}_6\text{F}_5)$), 140.2 (dm, J_{CF} = 252 Hz, $\text{B}(\text{C}_6\text{F}_5)$), 148.4 (dm, J_{CF} = 242 Hz, $\text{B}(\text{C}_6\text{F}_5)$), 192.9 (t, J_{CP} = 8.9 Hz, *cis* CO's), 195.0 (t, J_{CP} = 7.2 Hz, *trans* CO), 298.9 (s, *CHOB*). ^{31}P NMR (RT, 121 MHz, CD_2Cl_2): δ = 12.6 ppm (s). ^{19}F NMR (RT, 471 MHz, CD_2Cl_2): δ = -132.1 (6F, m, *ortho*- C_6F_5), -159.4 (3F, m, *para*- C_6F_5), -165.2 (6F, m, *meta*- C_6F_5). HRMS (FAB+) m/z calcd for $\text{C}_{52}\text{H}_{31}\text{BF}_{10}\text{O}_4\text{P}_2\text{Re}$ ($\text{M}-\text{C}_6\text{F}_5$) 1169.119, found 1169.121; for $\text{C}_{40}\text{H}_{30}\text{O}_4\text{P}_2\text{Re}$ ($\text{M}-\text{B}(\text{C}_6\text{F}_5)_3-\text{H}$) 823.1177, found 823.1798.

Synthesis of $\text{Mn}(\text{CO})_3(\text{PPh}_3)_2(\text{CHOB}\text{F}_3)$ (19). In the glovebox, a suspension of $[\text{Mn}(\text{CO})_4(\text{PPh}_3)_2][\text{BF}_4]$ (0.331 g, 0.4253 mmol) in THF (3 mL) was stirred in a vial. LiHBEt_3 (1 M in THF, 425 μL , 1 equiv.) was syringed in to give a yellow solution after filtration. $\text{BF}_3\cdot\text{OEt}_2$ (70 μL , 0.5529 mmol, 1.3 equiv.) was syringed into the THF solution

and stirred for 5 minutes, after which the solvent was evacuated. The solid was recrystallized from THF / petroleum ether to give 0.204 g of a yellow crystalline solid in 63 % yield. Anal. Calcd for $C_{40}H_{31}BF_3MnO_4P_2$: C, 62.93; H, 4.49. Found: C, 62.86; H, 4.22. 1H NMR (RT, 300 MHz, CD_2Cl_2): δ = 7.38 – 7.58 (30H, m, *ArH*), 12.80 (1H, s, *CHOB* F_3). ^{13}C NMR (RT, 126 MHz, CD_2Cl_2) partial: δ = 129.4 (t, J_{CP} = 5.0 Hz, *Ar*), 131.2 (s, *Ar*), 133.4 (t, J_{CP} = 5.2 Hz, *Ar*), 134.5 (d, J_{CP} = 44.5 Hz, *Ar*), 218.2 (t, J_{CP} = 18.2 Hz, *cis* CO's), 220.9 (t, J_{CP} = 16.5 Hz, *trans* CO), could not observe carbene carbon. ^{31}P NMR (RT, 121 MHz, CD_2Cl_2): δ = 63.2 ppm (s). ^{19}F NMR (RT, 471 MHz, CD_2Cl_2): δ = -156.3 ppm (s).

Synthesis of $Mn(CO)_3(PPh_3)_2(CHOB(C_6F_5)_3)$ (20). In the glovebox, a suspension of $[Mn(CO)_4(PPh_3)_2][BF_4]$ (0.095 g, 0.1221 mmol) in toluene (3 mL) was stirred in a vial. $NaHBEt_3$ (1 M in toluene, 122 μ L, 1 equiv.) was syringed in to give a yellow solution after filtration. $B(C_6F_5)_3$ (0.062 g, 0.1221 mmol) was dissolved in toluene (5 mL) and added to the reaction mixture and stirred for 5 minutes, after which the solvent was evacuated. The solid was recrystallized from CH_2Cl_2 / petroleum ether to give 0.095 g of a yellow crystalline solid in 65 % yield. Anal. Calcd. for $C_{58}H_{31}BF_{15}MnO_4P_2$: C, 57.83; H, 2.59. Found: C, 57.79; H, 3.04. 1H NMR (RT, 300 MHz, CD_2Cl_2): δ = 7.29 – 7.48 (30H, m, *ArH*), 13.22 (1H, s, *CHOB*(C_6F_5) $_3$). ^{13}C NMR (RT, 126 MHz, CD_2Cl_2) partial: δ = 130.2 (t, J_{CP} = 5.3 Hz, *Ar*), 132.8 (s, *Ar*), 133.1 (t, J_{CP} = 5.3 Hz, *Ar*), 134.1 (*Ar*), 137.1 (m, $B(C_6F_5)$), 148.6 (m, $B(C_6F_5)$), 212.4 (m, *cis* CO's), could not observe carbene carbon. ^{31}P NMR (RT, 121 MHz, CD_2Cl_2): δ = 64.8 ppm (s). ^{19}F NMR (RT, 471 MHz, CD_2Cl_2): δ = -132.2, -159.2, -165.2.

Synthesis of $[\text{Re}(\text{CO})_4(\text{PPh}_3)_2][\text{BPh}_4]$ (22). $[\text{Re}(\text{CO})_4(\text{PPh}_3)_2][\text{BF}_4]$ (0.167 g, 0.1894 mmol) and NaBPh_4 (0.097 g, 0.2834 mmol, 1.5 equiv.) were placed in a 80 mL flask, and CH_2Cl_2 (30 mL) was then added. The mixture was stirred for 3 days. The mixture was then filtered and the solvent removed in vacuo. The resulting residue was recrystallized from CH_2Cl_2 / petroleum ether to give 0.203 g of a white crystalline solid in 96 % yield. ^1H NMR (RT, 300 MHz, CD_2Cl_2): δ = 6.82 – 6.89 (4H, m, $\text{B}(\text{C}_6\text{H}_5)_4^-$), 6.98 – 7.05 (8H, m, $\text{B}(\text{C}_6\text{H}_5)_4^-$), 7.27 – 7.34 (8H, m, $\text{B}(\text{C}_6\text{H}_5)_4^-$), 7.43 – 7.52 (12H, m, Ar-*H*), 7.53 – 7.59 (18H, m, Ar*H*). ^{13}C NMR (RT, 126 MHz, CD_2Cl_2): δ = 122.3 (s, BPh_4^-), 126.2 (m, BPh_4^-), 130.2 (t, J_{PC} = 5 Hz, PPh_3), 132.2 (m, PPh_3), 132.8 (s, PPh_3), 133.1 (t, J_{PC} = 6 Hz), 136.4 (m, BPh_4^-), 164.6 (m, BPh_4^-), 186.2 (t, J_{PC} = 8 Hz, CO). ^{31}P NMR (RT, 121 MHz, CD_2Cl_2): δ = 4.1 ppm (s). HRMS (FAB+) m/z calcd for $\text{C}_{40}\text{H}_{30}\text{P}_2\text{O}_4\text{Re}$ 823.1177, found 823.1183.

NMR scale preparation of $[\text{Re}(\text{CO})_3(\text{PPh}_3)_2(\text{CHOTMS})][\text{BPh}_4]$ (23). In the glovebox, a suspension of $[\text{Re}(\text{CO})_4(\text{PPh}_3)_2][\text{BPh}_4]$ (0.011 g, 0.00987 mmol) in THF (3 mL) was stirred in a vial. LiHBEt_3 (1 M in THF, 10 μL , 1 equiv.) was syringed in to give a yellow solution. THF was evacuated to give the crude formyl species and LiBPh_4 byproduct as a yellow residue. The residue was dissolved in CD_2Cl_2 (0.4 mL) and transferred to a J-Young NMR tube and the solution frozen in the cold well. TMSOTf (2 μL , 0.00987 mmol, 1 equiv.) was dissolved in CD_2Cl_2 (0.3 mL) and the resulting solution added to J-Young tube and frozen in the cold well. The content of the tube was kept at LN_2 temperature until ready to be placed into the NMR probe, where it was thawed and shaken vigorously to give a yellow solution. ^1H NMR (RT, 300 MHz, CD_2Cl_2): δ = -0.09

(9H, s, OSi(CH₃)₃), 6.83 – 6.90 (4H, m, B(C₆H₅)₄[−]), 6.98 – 7.07 (8H, m, B(C₆H₅)₄[−]), 7.27 – 7.36 (8H, m, B(C₆H₅)₄[−]), 7.37 – 7.47 (12H, m, Ar-*H*), 7.48 – 7.56 (18H, m, Ar*H*), 13.91 (1H, s, CHOTMS). ³¹P NMR (RT, 121 MHz, CD₂Cl₂): δ = 11.3 ppm (s).

Synthesis of [Re(CO)₃(PPh₃)₂(CHOMe)][BPh₄] (24). In the glovebox, a suspension of [Re(CO)₄(PPh₃)₂][BPh₄] (0.079 g, 0.07091 mmol) in THF (3 mL) was stirred in a vial. LiHBEt₃ (1 M in THF, 71 μL, 1 equiv.) was syringed in to give a yellow solution. THF was evacuated to give the crude formyl species and LiBPh₄ byproduct as a yellow residue. CH₃OTf (8 μL, 0.07091 mmol, 1 equiv.) was dissolved in CH₂Cl₂ (5 mL) and added to the residue and stirred for 5 minutes, after which the solvent was evacuated. The solid was recrystallized from CH₂Cl₂ / petroleum ether to give 0.058 g of a white-yellow crystalline solid in 72 % yield. ¹H NMR (RT, 300 MHz, THF-*d*₈): δ = 3.30 (3H, s, OCH₃), 6.81 – 6.90 (4H, m, B(C₆H₅)₄[−]), 6.97 – 7.07 (8H, m, B(C₆H₅)₄[−]), 7.27 – 7.35 (8H, m, B(C₆H₅)₄[−]), 7.37 – 7.47 (12H, m, Ar-*H*), 7.48 – 7.57 (18H, m, Ar*H*), 11.94 (1H, s, CHOMe). ¹³C NMR (RT, 126 MHz, CD₂Cl₂): δ = 77.5 (s, CHOCH₃), 129.8 (t, *J*_{CP} = 5.4 Hz, Ar), 132.0 (s, Ar), 133.2 (t, *J*_{CP} = 5.9 Hz, Ar), 134.1 (t, *J*_{CP} = 26.1 Hz, Ar), 191.5 (m, *cis* CO's), 195.3 (m, *trans* CO), 303.9 (s, CHOMe). ³¹P NMR (RT, 121 MHz, THF-*d*₈): δ = 11.6 ppm (s). HRMS (FAB+) *m* / *z* calcd for C₄₁H₃₄O₄P₂Re 839.1490, found 839.1465.

Synthesis of [Mn(CO)₃(PPh₃)₂(CHOCH₃)][OTf] (25). In the glovebox, a suspension of [Mn(CO)₄(PPh₃)₂][BF₄] (0.204 g, 0.2621 mmol) in toluene (3 mL) was cooled down in the cold well. NaHBEt₃ (1 M in toluene, 262 μL, 1 equiv.) was then syringed in the cold vial to give a brownish mixture. In a separate vial was prepared a solution of CH₃OTf (30

μL , 0.2621 mmol, 1 equiv.) in toluene (4 mL), which was then added to the brown residue and stirred for 5 minutes. Volatiles were then removed in vacuo to give a yellow-brown solid. The residue was dissolved in CH_2Cl_2 and filtered through a Celite pad. The resulting yellowish solid was recrystallized twice from CH_2Cl_2 / petroleum ether to give 0.185 g of pure **25** as a yellow crystalline solid in 82 % yield. ^1H NMR (RT, 300 MHz, CH_2Cl_2): δ = 3.46 (3H, s, OCH_3), 7.45 – 7.57 (30H, m, Ar-*H*), 11.83 (1H, s, CHOMe). ^{13}C NMR (RT, 126 MHz, CD_2Cl_2): δ = 77.5 (s, CHOCH_3), 129.9 (t, J_{CP} = 5.2 Hz, Ar), 131.9 (s, Ar), 133.1 (t, J_{CP} = 5.2 Hz, Ar), 133.8 (t, J_{CP} = 45.0 Hz, Ar), 217.0 (t, J_{CP} = 17.7 Hz, *cis* CO's), 220.2 (t, J_{CP} = 17.7 Hz, *trans* CO), 338.5 (s, CHOMe). ^{31}P NMR (RT, 121 MHz, CH_2Cl_2): δ = 60.6 ppm (s). ^{19}F NMR (RT, 471 MHz, CD_2Cl_2): δ = -79.3 ppm (s, OTf). HRMS (FAB+) m/z for $\text{C}_{41}\text{H}_{34}\text{MnO}_4\text{P}_2$ 707.1313, found 707.1311.

Synthesis of $\text{Mn}(\text{CO})_3(\text{PPh}_3)_2(\text{CH}_2\text{OCH}_3)$ (26). In a vial, $[\text{Mn}(\text{CO})_3(\text{PPh}_3)_2(\text{CHOMe})][\text{OTf}]$ (0.040 g, 0.04669 mmol) was suspended in THF (2 mL). LiHBEt_3 (1 M in THF, 47 μL , 1 equiv.) was syringed into the vial. After 2 minutes of mixing followed by filtration, the resulting yellow solution was placed into a small vial, which was in turn placed in a larger vial containing petroleum ether (5 mL) for crystallization by diffusion. 15 hours later, the long yellow needles were decanted, washed with petroleum ether and dried under vacuum to give 0.025 g of **26** in 76 % yield. Anal. Calcd. for $\text{C}_{41}\text{H}_{35}\text{MnO}_4\text{P}_2$: C, 69.20; H, 5.38. Found: C, 68.96; H, 5.17. ^1H NMR (RT, 300 MHz, C_6D_6): δ = 2.73 (3H, s, OCH_3), 3.60 (2H, t, J_{HP} = 7.6 Hz, CH_2), 6.93 – 7.01 (6H, m, Ar-*H*), 7.02 – 7.11 (12H, m, Ar-*H*), 7.87 – 7.97 (12H, m, Ar-*H*). ^{13}C NMR (RT, 126 MHz, CD_2Cl_2): δ = 63.8 (s, OCH_3), 75.3 (t, J_{CP} = 12.9 Hz, CH_2OMe), 128.6 (t,

$J_{\text{CP}} = 4.6 \text{ Hz, Ar}$), 129.9 (s, Ar), 133.9 (t, $J_{\text{CP}} = 5.1 \text{ Hz, Ar}$) 136.7 (m, Ar), 222.8 (t, $J_{\text{CP}} = 17.8 \text{ Hz, trans CO}$), 224.4 (t, $J_{\text{CP}} = 21.3 \text{ Hz, cis CO's}$). ^{31}P NMR (RT, 121 MHz, C_6D_6): $\delta = 76.6 \text{ ppm (s)}$. ^{19}F NMR (RT, 471 MHz, C_6D_6): no signal, confirming the absence of OTf. IR: ν_{CO} (cm^{-1} , CH_2Cl_2) 2009, 1921, 1885.

Synthesis of *cis*-Mn(CO)₄(PPh₃)(CH₂OCH₃) (28**).** In the glovebox, Na/Hg (0.5% wt, 4 equiv.) was prepared in a flask. A THF (20 mL) solution of Mn(PPh₃)(CO)₄Br (0.388 g, 0.7620 mmol) was slowly added onto the amalgam. The mixture was allowed to stir in the absence of light for 2 hrs. In another flask, ClCH₂OCH₃ (58 μL , 1 equiv.) was dissolved in THF (10 mL) and placed in a Schlenk tube. On the Schlenk line, the manganese solution was decanted into the ClCH₂OCH₃ solution using a filter-tipped canula. The mixture was allowed to stir in the absence of light for 2 hrs, after which all volatiles were removed. The residue was dissolved in THF, filtered and recrystallized from THF / petroleum ether and dried under vacuum to give 0.319 g of **28** as a yellow crystalline solid in 88 % yield. ^1H NMR (RT, 300 MHz, C_6D_6): $\delta = 3.11$ (3H, s, OCH₃), 3.90 (2H, d, $J_{\text{HP}} = 7.0 \text{ Hz, CH}_2$), 6.93 – 7.02 (9H, m, Ar-*H*), 7.50 – 7.59 (6H, m, Ar-*H*). ^{13}C NMR (RT, 126 MHz, CD_2Cl_2): $\delta = 63.4$ (s, OCH₃), 71.1 (t, $J_{\text{CP}} = 11.7 \text{ Hz, CH}_2\text{OMe}$), 128.8 (d, $J_{\text{CP}} = 9.5 \text{ Hz, Ar}$), 130.6 (s, Ar), 133.4 (d, $J_{\text{CP}} = 10.4 \text{ Hz, Ar}$) 133.8 (d, $J_{\text{CP}} = 40.3 \text{ Hz, Ar}$), 215.7 (CO), 218.4 (d, $J_{\text{CP}} = 21.8 \text{ Hz, CO}$), 218.8 (CO). ^{31}P NMR (RT, 121 MHz, C_6D_6): $\delta = 61.2 \text{ ppm (s)}$. HRMS (FAB+) m/z calcd for $\text{C}_{24}\text{H}_{23}\text{MnO}_5\text{P}$ (M+H- H_2) 473.0351, found 473.0373.

Carbonylation of $\text{Mn}(\text{CO})_3(\text{PPh}_3)_2(\text{CH}_2\text{OCH}_3)$. To a flask was added $\text{Mn}(\text{CO})_3(\text{PPh}_3)_2(\text{CH}_2\text{OCH}_3)$ (0.150 g, 0.2117 mmol) and dissolved in C_6H_6 (20 mL). The flask was degassed on the Schlenk line and then filled with CO (1 atm). The flask was sealed and allowed to stir for 7 days protected from light. After removing all volatiles, the resulting yellow oil was triturated several times with hexanes and dried *in vacuo* to give 0.140 g of a yellow solid in 93% yield. The composition of the solid is a mixture containing *cis*- $\text{Mn}(\text{PPh}_3)(\text{CO})_4(\text{C}(\text{O})\text{CH}_2\text{OCH}_3)$ (80%), *trans*- $\text{Mn}(\text{PPh}_3)(\text{CO})_4(\text{C}(\text{O})\text{CH}_2\text{OCH}_3)$ (13%), and $\text{Mn}(\text{PPh}_3)(\text{CO})_4(\text{CH}_2\text{OCH}_3)$ (7%). *cis*- $\text{Mn}(\text{PPh}_3)(\text{CO})_4(\text{C}(\text{O})\text{CH}_2\text{OCH}_3)$: ^1H NMR (RT, 300 MHz, C_6D_6): δ = 3.17 (3H, s, OCH_3), 3.60 (2H, s, CH_2), 6.98 - 7.07 (m, *ArH*), 7.35 - 7.44 (m, *ArH*), 7.59 - 7.67 (m, *ArH*). ^{13}C NMR (RT, 126 MHz, C_6D_6): δ = 58.9 (s, OCH_3), 90.5 (d, J_{CP} = 3.0 Hz, CH_2), 128.6, 130.8, 134.0, 135.1, 322.6 (CO), 215.6 (CO), 217.7 (CO), 272.3 (dt, J_{CP} = 16.2 Hz, J_{CC} = 3.5 Hz, $\text{C}(\text{O})\text{CH}_2\text{OMe}$). ^{31}P NMR (RT, 121 MHz, C_6D_6): δ = 53.5 ppm (s, br). IR ν_{CO} (cm^{-1} , CH_2Cl_2) 2070, 1994, 1962, 1920, 1624. HRMS (FAB+) m/z for $\text{C}_{25}\text{H}_{21}\text{MnO}_6\text{P}$ (M+H) 503.0456, found 503.0465. *trans*- $\text{Mn}(\text{PPh}_3)(\text{CO})_4(\text{C}(\text{O})\text{CH}_2\text{OCH}_3)$: ^1H NMR (RT, 300 MHz, C_6D_6): δ = 3.27 (3H, s, OCH_3), 3.94 (2H, s, CH_2), 6.98 - 7.07 (m, *ArH*), 7.71 - 7.80 (m, *ArH*), 7.80 - 7.88 (m, *ArH*). ^{13}C NMR (RT, 126 MHz, C_6D_6): δ = 59.1 (s, OCH_3), 91.6 (d, J_{CP} = 4.6 Hz, CH_2), 128.8, 132.7, 135.6, 263.4 (br, $\text{C}(\text{O})\text{CH}_2\text{OMe}$), terminal CO's could not be observed as they were overlapping with with other peaks. IR ν_{CO} (cm^{-1} , CH_2Cl_2) 1636, other stretches could not be observed due to overlapping stretches.

References

-
- 1) Henrici-Olivé, G.; Olivé, S. In *The Chemistry of the Catalyzed Hydrogenation of Carbon Monoxide*; Springer-Verlag: New York, NY, 1984.
 - 2) Han, S.; Chang, C. D. In *Kirk-Othmer Encyclopedia of Chemical Technology*; Wiley & Sons, Inc: 2001.
 - 3) Fischer, F.; Tropsch, H. *Brennst. Chem.* **1926**, 7, 97.
 - 4) Collman, J. P.; Hegedus, L. S.; Norton, J. R.; Finke, R. G. In *Principles and Applications of Organometallic Chemistry*; University Science Books: Sausalito, CA, 1987.
 - 5) Levenspiel, O. *Ind. Eng. Chem. Res.* **2005**, 44, 5073.
 - 6) Khodakov, A. Y.; Chu, W.; Fongarland, P. *Chem. Rev.* **2007**, 107, 1692.
 - 7) Falbe, J., Ed. In *Chemierohstoffe aus Kohle*; Georg Thieme Verlag: Stuttgart, Germany, 1977.
 - 8) a) Argauer, R. J.; Landolt, G. R. US 3,702,886 (Mobil Oil Corporation), 1972. b) Kokotailo, G. T.; Lawton, S. L.; Olson, D. H.; Meier, W. M. *Nature* **1978**, 272, 437. c) Olson, D. H.; Kokotailo, G. T.; Lawton, S. L. *J. Phys. Chem.* **1981**, 85, 2238.
 - 9) Rothke, J. W.; Feder, H. M. *J. Am. Chem. Soc.* **1978**, 100, 3623.
 - 10) Bradley, J. *J. Am. Chem. Soc.* **1979**, 101, 7419.
 - 11) Dombek, B. D. *J. Am. Chem. Soc.* **1980**, 102, 6855.
 - 12) Shoer, L. I.; Schwartz, J. *J. Am. Chem. Soc.* **1977**, 99, 5831.
 - 13) Spessard, G. O.; Miessler, G. L. In *Organometallic Chemistry*; Prentice Hall: Upper Saddle River, NJ, 1997.
 - 14) Pruett, R. L.; Walker, W. E. (Union Carbide Corp.), German Offen. 2262318, 1973; US 210538, 1971.
 - 15) Wolczanski, P. T.; Bercaw, J. E. *Acc. Chem. Res.* **1980**, 13, 121.
 - 16) Manriquez, J. M.; Sanner, R. D.; Marsh, R. E.; Bercaw, J. E. *J. Am. Chem. Soc.* **1976**, 98, 6733.

-
- 17) Manriquez, J. M.; McAlister, D. R.; Sanner, R. D.; Bercaw, J. E. *J. Am. Chem. Soc.* **1978**, *100*, 2716.
 - 18) Wolczanski, P. T.; Threlkel, R. S.; Bercaw, J. E. *J. Am. Chem. Soc.* **1979**, *101*, 218.
 - 19) Barger, P. T. Ph.D. Thesis, California Institute of Technology, Pasadena, CA, 1983.
 - 20) Dombek, B. D. *Adv. Catal.* **1983**, *32*, 325.
 - 21) Costa, L. C. *Catal. Rev.-Sci. Eng.* **1983**, *25*, 325.
 - 22) Keim, W. In *Catalysis in C₁ Chemistry*; Keim, W., Ed.; D. Reidel: Boston, 1983.
 - 23) Herrmann, W. A. *Angew. Chem. Int. Ed.* **1982**, *21*, 117.
 - 24) Cutler, A. R.; Hanna, P. K.; Vites, J. C. *Chem. Rev.* **1988**, *88*, 1363.
 - 25) Collman, J. P.; Winter, S. R. *J. Am. Chem. Soc.* **1973**, *95*, 4089.
 - 26) Casey, C. P.; Andrews, M. A.; McAlister, D. R.; Rinz, J. E. *J. Am. Chem. Soc.* **1980**, *102*, 1927.
 - 27) Tam, W.; Lin, G.-Y.; Wong, W.-K.; Kiel, W.-A.; Wong, V. K.; Gladysz, J. A. *J. Am. Chem. Soc.* **1982**, *104*, 141.
 - 28) Sweet, J. R.; Graham, W. A. G. *J. Am. Chem. Soc.* **1982**, *104*, 2811.
 - 29) Miedaner, A.; DuBois, D. L.; Curtis, C. J.; Haltiwanger, R. C. *Organometallics* **1993**, *12*, 299.
 - 30) Weiner, W. P.; Hollander, F. J.; Bergman, R. G. *J. Am. Chem. Soc.* **1984**, *106*, 7462.
 - 31) Wayland, B. B.; Woods, B. A.; *J. Chem. Soc., Chem. Commun.* **1981**, 700.
 - 32) Fagan, P. J.; Moloy, K. G.; Marks, T. J. *J. Am. Chem. Soc.* **1981**, *103*, 6959.
 - 33) Casey, C. P.; Andrews, M. A.; Rinz, J. E. *J. Am. Chem. Soc.* **1979**, *101*, 741.
 - 34) Tam, W.; Wong, W.-K.; Strouse, C. E.; Gladysz, J. A.; *J. Am. Chem. Soc.* **1979**, *101*, 1589.
 - 35) Gibson, D. H.; Owens, K.; Mandal, S. K.; Sattich, W. E.; Franco, J. O. *Organometallics* **1989**, *8*, 498.

-
- 36) Gibson, D. H.; Mandal, S. K.; Owens, K.; Richardson, J. F. *Organometallics* **1990**, 9, 1936.
- 37) Gibson, D. H.; Owens, K.; Mandal, S. K.; Sattich, W. E.; Franco, J. O. *Organometallics* **1991**, 10, 1203.
- 38) Gibson, D. H.; Mandal, S. K.; Owens, K.; Richardson, J. F. *Organometallics* **1987**, 6, 2624.
- 39) Berning, D. E.; Miedaner, A.; Curtis, C. J.; Noll, B. C.; Rakowski DuBois, M. C.; DuBois, D. L. *Organometallics* **2001**, 20, 1832.
- 40) Curtis, C. J.; Miedaner, A.; Ellis, W. W.; DuBois, D. L. *J. Am. Chem. Soc.* **2002**, 124, 1918.
- 41) Price, A. J.; Ciancanelli, R.; Noll, B. C.; Curtis, C. J.; DuBois, D. L.; Rakowski DuBois, M. *Organometallics* **2002**, 21, 4833.
- 42) DuBois, D. L.; Blake, D. M.; Miedaner, A.; Curtis, C. J.; DuBois, M. R.; Franz, J. A.; Linehan, J. C. *Organometallics* **2006**, 25, 4414.
- 43) Herrmann, W. A.; Plank, J. *Angew. Chem., Int. Ed. Engl.* **1978**, 17, 525.
- 44) Herrmann, W. A.; Plank, J.; Ziegler, M. L.; Weidenhammer, K. *J. Am. Chem. Soc.* **1979**, 101, 3133.
- 45) Fischer, H. *Angew. Chem., Int. Ed. Engl.* **1983**, 22, 874.
- 46) Bodnar, T. W.; Cutler, A. R. *J. Am. Chem. Soc.* **1983**, 105, 5926.
- 47) Gibson, S. E.; Ward, M. F.; Kipps, M.; Stanley, P. D.; Worthington, P. A. *Chem. Commun.* **1996**, 263.
- 48) Grotjahn, D. B.; Bikzanova, G. A.; Collins, L. S. B.; Concolino, T.; Lam, K.-C.; Rheingold, A. L. *J. Am. Chem. Soc.* **2000**, 122, 5222.
- 49) Wong, W. K.; Tam, W.; Strouse, C. E.; Gladysz, J. A. *J. Chem. Soc. Chem. Commun.* **1979**, 530.
- 50) Bleeke, J. R.; Rausher, D. J.; Moore, D. A. *Organometallics* **1987**, 6, 2614.
- 51) Bleeke, J. R.; Earl, P. L. *Organometallics* **1989**, 8, 2735.
- 52) Brown, D. A.; Mandal, S. K.; Ho, D. M.; Becker, T. M. *J. Organometal. Chem.* **1999**, 592, 61.

-
- 53) Kowalczyk, J. J.; Arif, A. M.; Gladysz, J. A. *Chem. Ber.* **1991**, *124*, 729.
- 54) Kiel, W. A.; Lin, G.-Y.; Constable, A. G.; McCormick, F. B.; Strouse, C. E.; Eisenstein, O.; Gladysz, J. A. *J. Am. Chem. Soc.* **1982**, *104*, 4865.
- 55) Chen, J.; Yu, Y.; Liu, K.; Wu, G.; Zheng, P. *Organometallics* **1993**, *12*, 1213.
- 56) Frech, C. M.; Blacque, O.; Schmalke, H. W.; Berke, H.; Adlhart, C.; Chen, P. *Chem. Eur. J.* **2006**, *12*, 3325.
- 57) Ruszczyk, R. J.; Huang, B.-L.; Atwood, J. D. *J. Organomet. Chem.* **1986**, *299*, 205.
- 58) Kuchynka, D. J.; Amatore, C.; Kochi, J. K. *Inorg. Chem.* **1986**, *25*, 4087.
- 59) Miller, A. J. M.; Labinger, J. A.; Bercaw, J. E. *J. Am. Chem. Soc.*, submitted for publication.
- 60) Welch, G. C.; Stephan, D. W. *J. Am. Chem. Soc.* **2007**, *129*, 1880.
- 61) Gomez-Gallego, M.; Mancheno, M. J.; Sierra, M. A. *Acc. Chem. Res.* **2005**, *38*, 44.
- 62) Sierra, M. A.; del Amo, J. C.; Mancheno, M. J.; Gomez-Gallego, M. *J. Am. Chem. Soc.* **2001**, *123*, 851.
- 63) Gibson, D. H.; Mandal, S. K.; Owens, K.; Sattich, W. E.; Franco, J. O. *Organometallics* **1989**, *8*, 1114.
- 64) Cawse, J. N.; Fiato, R. A.; Pruett, R. L. *J. Organomet. Chem.* **1979**, *172*, 405 and references cited therein.
- 65) Butts, S. B.; Strauss, S. H.; Holt, E. M.; Stimson, R. E.; Alcock, N. W.; Shriver, D. F. *J. Am. Chem. Soc.* **1980**, *102*, 5093.
- 66) Flood, T. C.; Jensen, J. E.; Statler, J. A. *J. Am. Chem. Soc.* **1981**, *103*, 4410.
- 67) Brinkman, K. C.; Vaughn, G. D.; Gladysz, J. A. *Organometallics* **1982**, *1*, 1056.
- 68) Andersen, J.-A. M.; Moss, J. R. *Organometallics* **1994**, *13*, 5013.
- 69) Massick, S. M.; Mertens, V.; Marhenke, J.; Ford, P. C. *Inorg. Chem.* **2002**, *41*, 3553.
- 70) Wang, X.; Weitz, E. *J. Organomet. Chem.* **2004**, *689*, 2354.
- 71) Kraihanzel, C. S.; Maples, P. K. *Inorg. Chem.* **1968**, *7*, 1806.

-
- 72) For an analogous synthesis, see Hevia, E.; Miguel, D.; Pérez, J.; Riera, V. *Organometallics* **2006**, 25, 4909.
- 73) Noack, K.; Ruch, M.; Calderazzo, F. *Inorg. Chem.* **1968**, 7, 345.
- 74) Crowther, D. J.; Tivakornpannarai, S.; Jones, W. M. *Organometallics* **1990**, 9, 739. In this paper, an analogous acyl complex, $\text{Mn}(\text{PPh}_3)(\text{CO})_4(\alpha\text{-methoxycyclobutylacetyl})$ is discussed: *cis* (272.15 ppm, $J_{\text{CP}} = 14.5$ Hz); *trans* (264.3 ppm, coupling constant too small to be determined).
- 75) Tso, C. C.; Cutler, A. R. *Organometallics* **1986**, 5, 1834.
- 76) Levitre, S. A.; Cutler, A. R.; Forschner, T. C. *Organometallics* **1989**, 8, 1133.
- 77) Bond, A. M.; Colton, R.; McDonald, M. E. *Inorg. Chem.* **1978**, 17, 2842.
- 78) Angelici, R. J.; Basolo, F. *J. Am. Chem. Soc.* **1962**, 84, 2495.
- 79) Owen, J. S. Ph.D. Thesis, California Institute of Technology, Pasadena, CA, 2005.